



Cite this: DOI: 10.1039/d5me00045a

# The evolution of antifreeze proteins and the inspiration for the development of novel antifreeze materials

 Yihang Gao, <sup>a</sup> Caixia Han<sup>\*a</sup> and Jianjun Wang <sup>\*abc</sup>

Uncontrolled ice formation poses a significant problem in various industries from atmospheric physics to cryobiology. Therefore, ice controlling strategies including regulating ice nucleation and controlling ice recrystallization and growth are highly pursued. In nature, antifreeze proteins (AFPs) exist in many cold-acclimated species, which can effectively control the size and shape of ice crystals, thus minimizing the deleterious effects of ice. Understanding how nature has evolved AFPs to adapt organisms to cold environments is crucial for guiding the design of novel antifreeze materials by human beings. Herein, we critically reviewed the evolutionary models underlying the development of AFPs, including escape from adaptive conflict (EAC) (primarily involving type III AFPs and Antarctic antifreeze glycoproteins, AFGPs), *de novo* evolution (exemplified by Arctic codfish AFGPs), horizontal gene transfer (HGT) (represented by type II AFPs and the DUF3494 family), and convergent evolution (predominantly involving type I AFPs and AFGPs). Furthermore, strategies for designing and fabricating bio-inspired antifreeze materials that mirror these evolutionary processes are also discussed. We anticipate that the insights presented here will inspire and aid in the identification of material design strategies for the future development of novel antifreeze materials.

 Received 31st March 2025,  
 Accepted 18th June 2025

DOI: 10.1039/d5me00045a

[rsc.li/molecular-engineering](https://rsc.li/molecular-engineering)

## Design, System, Application

In multiple industrial sectors, such as food storage, cryomedicine, and cold-chain logistics, uncontrolled ice formation presents a pervasive and costly challenge. Antifreeze proteins (AFPs), naturally present in cold-acclimated organisms, play a pivotal role in regulating ice crystal size, shape, and growth, thereby minimizing the deleterious effects of ice on cellular structures and functions. This review offers an exhaustive exploration of the evolutionary processes that have driven the development of AFPs in cold environments. It critically examines key evolutionary models, including escape from adaptive conflict (EAC), *de novo* evolution, horizontal gene transfer (HGT), and convergent evolution, elucidating their respective contributions to the functional diversity of AFPs. By integrating insights from evolutionary biology into the realm of materials science, this review endeavors to inspire the rational design of advanced, bio-inspired antifreeze materials. It aims to transform the empirical strategies employed by nature in its evolutionary trial-and-error process into practical and actionable design principles, facilitating the innovation of novel antifreeze solutions tailored to meet the specific needs of various industries.

## 1. Introduction

Undesired ice formation including ice nucleation, ice growth and recrystallization poses a serious threat to our daily life across numerous fields, ranging from cryobiology to atmospheric physics. In cryobiology, cryopreservation aims to extend the storage times of biosamples. However, the formation and growth of ice crystals are extremely harmful to most biological systems, leading to ice damage and solution effects at the cellular level.<sup>1–4</sup> Besides cryobiology, in areas

like traffic, cables, and aerospace, uncontrolled ice formation on the substrate is also detrimental. For example, aircraft wings can cause a catastrophic event, threatening the safety of human beings.<sup>5</sup> A notable illustration is Continental Connection Flight 3407, which crashed on its way from Newark to Buffalo, primarily due to ice accretion on the wings, resulting in the loss of all lives on board.<sup>6</sup> In light of the above-mentioned risks and damage associated with ice formation in different scenarios, the design of antifreeze materials for cryopreservation applications and the development of anti-icing coatings are of high significance.

Antifreeze proteins (AFPs) are considered as the most efficient biological antifreeze agents. They were first discovered in 1969 (ref. 7) and have since been found to be widespread throughout various biological kingdoms, including insects, plants, fish, and microorganisms.<sup>8–19</sup> AFPs possess three crucial functions due to their ice-binding

<sup>a</sup> Interdisciplinary Research Center for Advanced Materials, Technical Institute of Physics and Chemistry, Chinese Academy of Sciences, Beijing 100190, China.

E-mail: hancaixia@mail.ipc.ac.cn, wangjianjun@mail.ipc.ac.cn

<sup>b</sup> School of Chemistry Sciences, University of Chinese Academy of Sciences, Beijing 100049, China

<sup>c</sup> Songshan Lake Materials Laboratory, Dongguan, Guangdong 523808, China

ability: thermal hysteresis (TH), dynamic ice shaping (DIS), and ice recrystallization inhibition (IRI). TH activity refers to the ability to lower the freezing point without affecting the melting point, resulting in a temperature gap between the freezing and melting points.<sup>20</sup> During this process, within the TH temperature gap, AFPs can change the shape or faceting of ice crystals, which is known as DIS activity.<sup>20</sup> IRI activity means the growth of large ice crystals based on smaller ones (a process also known as Oswald ripening).<sup>21</sup> This can help to reduce the free energy and make the system more stable. Therefore, AFPs enable the host organisms to survive under cold conditions by either depressing the freezing points or inhibiting ice recrystallization.

However, the application of AF(G)Ps is restricted by their toxicity, high cost and the sudden burst of ice crystal growth that occurs beyond the TH gap. To address these limitations, numerous efforts have been made to design AFP analogues by mimicking the structures or functions of AFPs through a process of trial and error.<sup>22–25</sup> To date, the most frequently employed methods heavily rely on a “black-box approach” with a few design rules. For instance, a vast candidate library was constructed consisting of  $2 \times 10^{10}$  randomly selected peptide sequences. Despite this extensive library, only one cyclic peptide with IRI activity was identified through ice-affinity selection.<sup>26</sup> In recent years, *in silico* technologies have gained widespread popularity in the design and identification of novel functional molecules. This includes the notable work of Purohit, in which a computational approach was implemented to search for deleterious mutations associated with cancer.<sup>27–32</sup> In the context of AFP analogues, it is common to examine whether they match the ice crystal lattice using *in silico* technologies.<sup>33–35</sup> This computational-based approach helps in better understanding the structure–function relationship of AFP analogues and their interaction with ice crystals. Nonetheless, the experimental trial-and-error approaches are often cumbersome. The development and optimization of more universal and effective methods for designing antifreeze materials are urgently desired.

Notably, the evolutionary history of AFPs can be regarded as a natural design process.<sup>36–43</sup> This process has led to distinct adaptations in different organisms. For example, many insects and other terrestrial arthropods have developed hyperactive AFPs (AFPs that possess a TH value of 2–13 °C), thus enabling them to avoid freezing and survive even at extreme sub-zero temperatures down to –20 °C.<sup>44–46</sup> In contrast, many plant AFPs have evolved excellent IRI activity, despite having a moderate TH value ranging from 0 to 2 °C. They can protect their host from mechanical damage caused by large ice crystals because of ice recrystallization that occurs when plant fluids freeze.<sup>14,15,47</sup> Currently, most researchers focus on drawing inspiration from the properties of AFPs for designing antifreeze materials, with limited attention given to incorporating insights from the evolutionary processes of AFPs.<sup>48</sup> Given the remarkable success of nature in evolving these proteins over time, leveraging the evolutionary principles of AFPs to guide the design of antifreeze materials holds significant potential for optimizing the development of such materials.

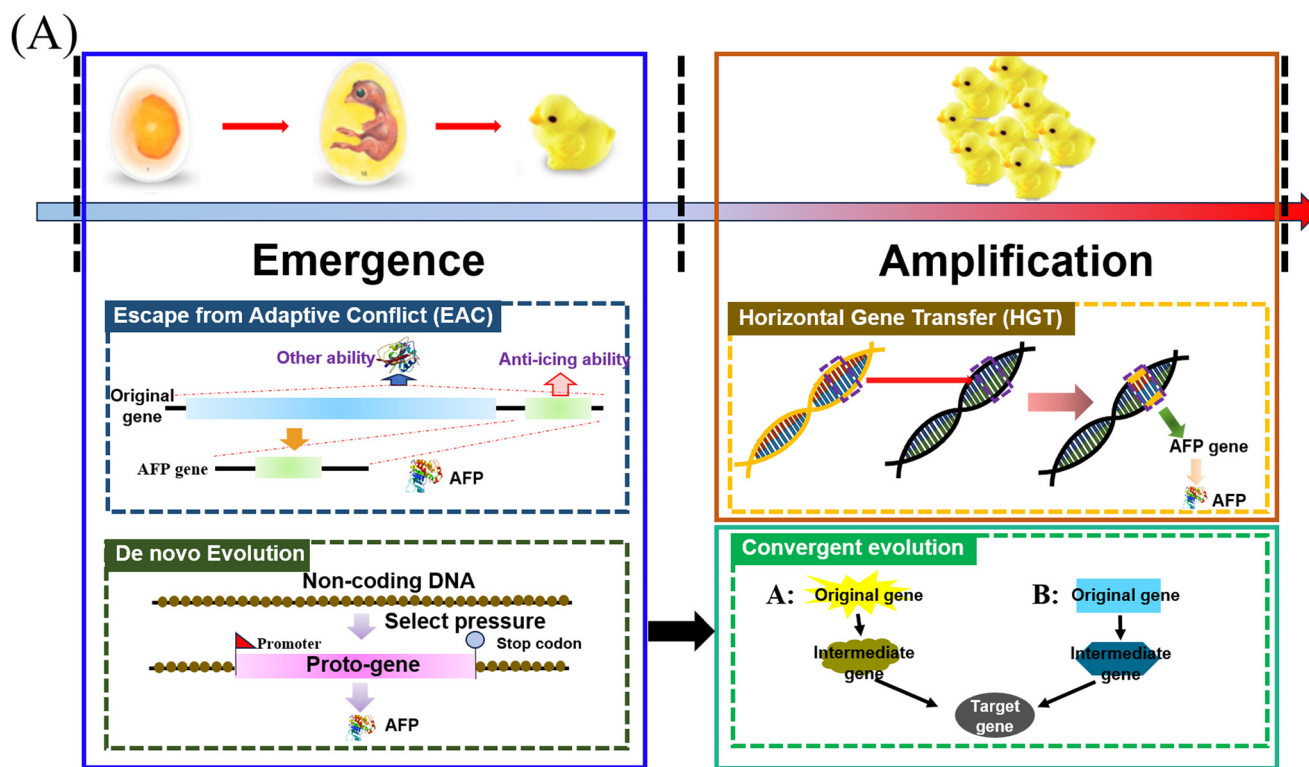
Nowadays, most reviews on the evolution of AFPs have all focused on a single type of AFP previously, such as the DUF3494 family (which is predominantly found in microorganisms)<sup>49</sup> or fish AFPs.<sup>50</sup> However, an overall understanding of the evolutionary histories of AFPs across all species is lacking, and it is necessary to gain such an understanding. In this review, we initially introduce the AFPs derived from all species. Subsequently, we systematically summarize and compare the evolutionary histories of AFPs from various organisms. We comprehensively categorize the evolutionary patterns of different AFPs into four evolutionary models based on their unique mechanisms of molecular origin: escape from adaptive conflict (EAC), *de novo* gene evolution, horizontal gene transfer (HGT) and convergent evolution (Fig. 1A). We introduce the concept of these evolutionary models and detailed discussions are conducted to investigate the evolutionary process of AFPs involving these evolutionary models. Furthermore, we bridge the gap between evolutionary biology and materials science by illustrating how these natural evolutionary paradigms have inspired the rational design of bio-inspired antifreeze materials, an approach that has not been proposed in the past (Fig. 1B). Therefore, this review serves dual objectives: on the one hand, it endeavors to deepen our understanding of how organisms have adapted to frigid environments through the evolution of AFPs. On the other hand, by presenting the natural trial-and-error process of AFP evolution, we hope to inspire and guide the development of novel antifreeze materials. Our synthesis aims to translate empirical observations of nature's trial-and-error processes into practical principles that can guide the innovation of antifreeze materials.

## 2. AFPs

AFPs have evolved across various species and are widely attractive because they enable their hosts to survive in subzero environments by inhibiting ice crystal growth and recrystallization. To date, AFPs have been discovered in many different branches of the tree of life, including fish, insects, plants, microorganisms, *etc.*<sup>51</sup> AFPs from different species exhibit remarkable diversity in their structures, functions, and evolutionary origins, reflecting the unique adaptations of different organisms to cold stress. Herein, we summarize different AFPs by species, including fish, insects, plants, and microorganisms.

### 2.1 Fish AFPs

Fish AFPs were first discovered in Antarctic fish species in 1969.<sup>52</sup> They are typically classified into four types: type I, type II, type III, and AFGPs. Type I AFPs are characterized by their  $\alpha$ -helical structure and preferentially bind to the pyramidal plane surfaces of ice crystals.<sup>9</sup> Type II AFPs, such as those from sea ravens, are globular proteins rich in cysteine residues and disulfide bridges.<sup>53</sup> Type III AFPs, like those from eelpouts, are also globular but bind to a different set of ice crystal planes.<sup>54</sup> AFGPs are found in both Arctic and Antarctic species, characterized by their unique repetitive



(B)

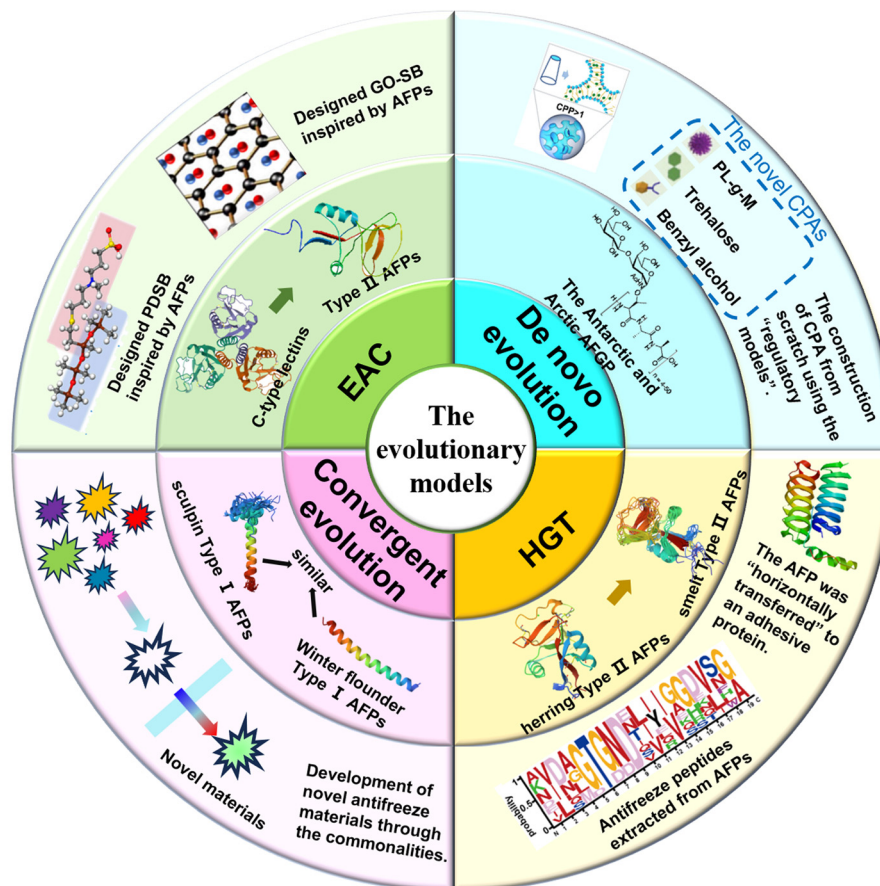


Fig. 1 (A) The mechanisms of the four evolutionary models. (B) The schematic of this review.

“Ala-Ala-Thr” sequence. In this sequence, the Thr residues are glycosylated, which enables AFGPs to bind to ice crystals and lower the freezing point of body fluids (Fig. 2A).<sup>55,56</sup>

## 2.2 Insect AFPs

Most AFPs secreted by terrestrial insects exhibit a hyperactive TH activity, such as *Tenebrio molitor* AFPs (*Tm*AFPs) and *Choristoneura fumiferana* AFPs (*Cf*AFPs). The powerful TH activity endows them with freeze tolerance even at  $-20\text{ }^{\circ}\text{C}$ .<sup>11</sup> Generally, *Tm*AFPs possess a right-handed  $\beta$ -helix structure and form ice-binding sites through tandem 12-residue repeats, resulting in a significant TH activity (Fig. 2A and B).<sup>58</sup> By contrast, *Cf*AFPs possess a left-handed helix conformation with triangular cross sections (Fig. 2A).<sup>13</sup> These different structures reflect their different evolutionary mechanisms.

## 2.3 Plant AFPs

Plants also produce AFPs, with *Lolium perenne* AFPs (*Lp*AFPs) and *Daucus carota* AFPs (*Dc*AFPs) being two well-studied examples.<sup>51,59</sup> *Lp*AFPs were produced by freeze-tolerant forage grass, exhibiting a left-handed helix structure and strong IRI activity, despite having a relatively low TH value.<sup>15</sup> Similarly, *Dc*AFPs found in carrots also display excellent IRI activity, which is crucial for their survival in cold climates (Fig. 2A).<sup>16</sup> In general, plant AFPs tend to show high IRI activities but low TH activities (Fig. 2B).<sup>50</sup> These characteristics can be attributed to their living environments in extremely cold regions where freezing is inevitable. By inhibiting ice crystal recrystallization, plant AFPs effectively help plants avoid mechanical damage caused by ice crystals.

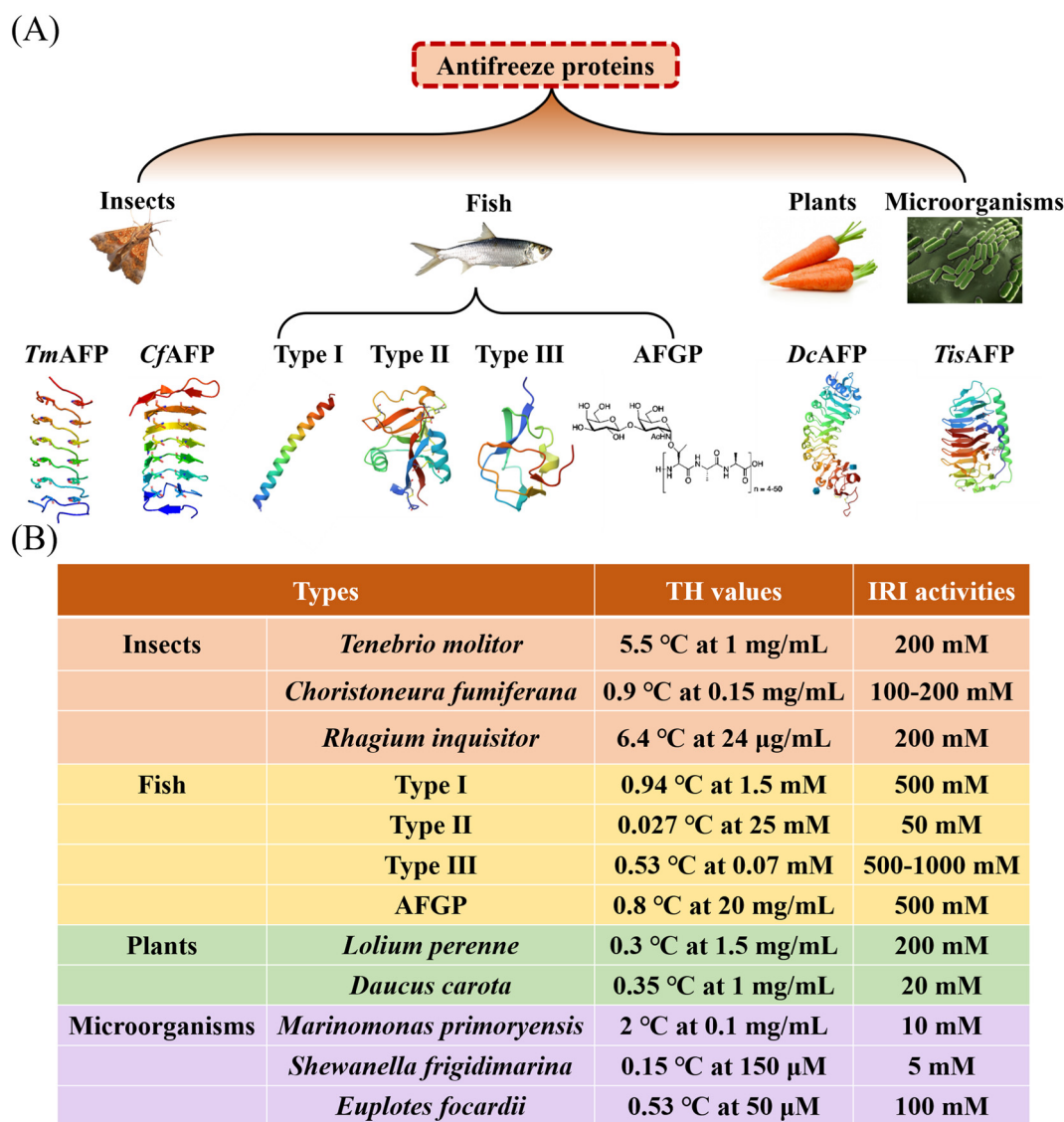


Fig. 2 (A) The representative AFPs. Insect AFPs (*Tenebrio molitor*; PDB ID: 1EZG, *Choristoneura fumiferana*; PDB ID: 1M8N). Fish AFPs (type I AFP; PDB ID: 1WFA, type II AFP; PDB ID: 2PY2, type III AFP; PDB ID: 1MSI, AFGP was reprinted with permission from ref. 57 Copyright (2010) Wiley). Plant AFPs (*Daucus carota*; PDB ID: 6W78), microorganism AFPs (*Typhula ishikariensis*; PDB ID: 5B5H). (B) The TH values and IRI activities of representative AFPs.

## 2.4 Microorganism AFPs

Many microorganisms, including bacteria and fungi, have also been reported to synthesize AFPs to survive in subzero environments. For instance, *Marinomonas primoryensis* AFP (MpAFP) is a notably large protein, comprising five distinct regions. Among these regions, one exhibits a pivotal role in antifreeze activity by virtue of its capacity to bind to ice crystals.<sup>60</sup> DUF3494 AFPs, which exhibit a widespread distribution across yeast, bacteria, and microalgae, are characterized by a discontinuous  $\beta$ -solenoid structure accompanied by an adjacent  $\alpha$ -helix. They are the largest antifreeze protein family which can also bind to ice crystals (Fig. 2A).<sup>61</sup>

In summary, antifreeze proteins have evolved independently across multiple species, each exhibiting unique structures and functions tailored to their specific cold environments. These proteins not only provide insights into the molecular mechanisms of cold adaptation but also hold great potential for applications in cryopreservation, anti-icing coatings, *etc.*<sup>51</sup>

## 3. The methodology for evolutionary studies

To investigate the evolutionary process of AFPs, the methodology is of great importance. To date, alignment of gene or cDNA sequences, the construction of phylogenetic trees and analysis of their topological structures, dot matrix analyses, chromosomal fluorescence *in situ* hybridization (FISH), *etc.* are all commonly used analytical methods. The application and development of these technologies contribute to a more comprehensive understanding of the evolutionary relationships among the AFPs.

### 3.1 Database

GenBank, EMBL, DDBJ, NCBI, UniProt, and Ensembl are all widely used databases in evolutionary studies.<sup>62–64</sup> In addition, when data are lacking in these databases, some researchers extract and sequence the DNA themselves. For instance, Graham *et al.* extracted genomic DNA from a diverse range of fish species caught along the Atlantic coast, the Pacific coast of Canada, and other pertinent locations. Then, they used the obtained sequences to construct a novel database to investigate the phylogenetic relationships among these fish.<sup>65</sup> Besides, Raymond *et al.* employed an Easy-DNA kit to isolate genomic DNA from a broad spectrum of organisms such as *Amphora* sp. and *Attheya* sp. Subsequently, they carried out research to probe into HGT events during the colonization of sea ice by algae.<sup>66</sup>

Aside from that, construction of bacterial artificial chromosome (BAC) libraries and phage libraries plays pivotal roles in studying biological evolution. They can efficiently maintain the integrity of large genomic DNA fragments and provide abundant genetic information for research. For instance, in a type III AFP evolutionary study, Deng *et al.*

constructed a BAC library using *Lycodichthys dearborni* caught from McMurdo Sound, Antarctica. Then the SAS and type III AFP clones were screened and sequenced from this library. Gene annotation was subsequently conducted using the BLAST algorithm, and the resulting sequence contigs were compared against the database maintained by the NCBI.<sup>67</sup> In an Arctic codfish AFGP evolutionary study, BAC libraries were also constructed for two AFGP-bearing gadids (*Boreogadus saida* and *Microgadus tomcod*) and the AFGP-lacking basal species (*Brosmius brosme*) as well as phage libraries for other three AFGP-lacking gadids, *Merlangius merlangus*, *Trisopterus esmarkii* and *Lota lota* to isolate and sequence the AFGP genomic regions for comparative evolutionary analysis.<sup>43</sup> Thereafter, Zhuang *et al.* revealed the order and manner in which the signal peptide, the TATA box and the main constituents of TAA tripeptide repeats appear.<sup>43</sup>

### 3.2 Sequence alignment

Sequence alignment is a commonly employed technique in evolutionary research. For instance, it serves as a prerequisite step before constructing phylogenetic trees.<sup>68</sup> Clustal Omega, T-Coffee, MEGA, *etc.* are all among the widely-used tools in this field.<sup>69–71</sup> By comparing the similarities and discrepancies within genomic or amino acid sequences, researchers are able to infer the direction of evolutionary change. For example, through sequence alignment of the introns and exons, it has been suggested that the AFGP in Antarctic notothenioid fishes was derived from trypsinogen protease. Besides, the evolutionary process has also been elaborated in detail.<sup>72,73</sup>

### 3.3 Phylogenetic analyses

Construction of phylogenetic trees depicts the relationships among different species or genes, which are one of the most commonly used methods for studying evolution. To date, there are primarily two main objectives for constructing phylogenetic trees to study the evolutionary relationships among AFPs: one is to investigate the evolutionary relationships among different species that produced AFPs (in this case, whole genomes or housekeeping genes of the species are generally used). The other is to specifically study the relationships among AFPs from different species (in this scenario, AFP sequences are specifically utilized). When it comes to constructing a phylogenetic tree, several parameters need to be taken into consideration: initially, it involves the construction of a phylogenetic tree model. The commonly used models include Bayesian, Neighbor-Joining (NJ), Maximum Likelihood (ML), *etc.* Additionally, the sequences used and the parameters employed should also be considered. Phylogenetic trees are the most commonly utilized tools in the analysis of HGT and convergent evolution. Herein, we summarize the data, evolutionary models, software, and corresponding parameters employed in studies involving HGT analysis and convergent evolution (Table 1).

**Table 1** The methodologies used for studying the evolutionary process of type II AFPs

	Ref.	Data	Evolutionary models	Software	Parameters	Validation/additional analyses
HGT	65	Type II AFP gene sequences obtained through PCR amplification and sequencing. 16S rRNA sequences used as a reference	Bayesian analysis, maximum parsimony, 16S rRNA sequence analysis	MrBayes, PAUP* version 4.0b10	Mixed model in MrBayes (1 000 000 generations, sampling every 100); GTR + I + G model for 16S rDNA	Validation of tree topology through bootstrap, Bayesian support, and comparison with 16S rDNA phylogeny
	74	Sequences of RBP3–2 protein and the smelt AFP gene obtained from fish genomic DNA and BAC clone sequencing	Maximum likelihood	MEGA5.01	Bootstrap support values (500 replicates)	Validation of tree topology through bootstrap support
	64	Type II AFP and AFLP gene sequences from teleosts, with additional sequences <i>via</i> targeted sequencing. Structurally related C-type lectin sequences included	Prunier analysis	DAMBE 5.2.57, MAFFT 6, Prunier 2.0, MEME, Datamonkey	Prunier “slow” and “fast” methods; MEME analysis	Validation of HGT events through statistical tests
	75	Amino acid sequences of AFP/AFLP genes and SSU rRNA sequences	GTR + $\Gamma$ 4 for SSU rRNA; J1, GTR, TVM for codon positions	BayesPhylogenies, Treefinder	Bayesian MCMC (3 runs, $2 \times 10^7$ generations, burnin 10%); LR-ELW, Kishino-Hasegawa, Shimodaira-Hasegawa tests	Validation of HGT through multiple statistical tests
	76	Amino acid sequences of ice-binding proteins and homologues from various taxa	WAG model for ML phylogeny	PhyML, PAUP*, MrBayes	Bootstrap support values (100 replicates); posterior probabilities (80 000 generations, four chains)	Validation of tree topology through bootstrap and Bayesian support
	77	Eukaryotic AFP transcripts from Arctic/Antarctic sea ice microbial communities; PfamA DUF3494 domain sequences	LG model for ML tree construction	pplacer, PhyML	Bootstrap values (1000 replicates); posterior probabilities (threshold 75%)	Validation of tree topology through bootstrap and Bayesian support
	78	IBP sequences from <i>Chloromonas brevispina</i> and related organisms	Not explicitly stated	Mega5, ClustalW, BioEdit	Bootstrap values (500 replications)	Validation of tree topology through bootstrap support
	66	IBP sequences and 18S rRNA sequences from sea ice algae and bacteria	Neighbor-joining method	Mega5, BioEdit	Bootstrap values (500 replications)	Validation of tree topology through bootstrap support
	79	Amino acid sequences of <i>Antarctomyces psychrotrophicus</i> IBPs and related microbial IBPs; 16S/18S rRNA sequences	ML for DUF3494 tree; neighbor-joining for rRNA tree; Bayesian inference (BI)	MEGA7, Clustal omega	Bootstrap values (500 replicates); posterior probabilities (BI); AU test, SH test	Validation of tree topology through bootstrap, Bayesian support, and statistical tests
	80	cDNA and genomic sequences of AFP isoforms from <i>Tenebrio molitor</i> and <i>Dendroides canadensis</i> beetles	ML, MP	ClustalX, PAUP*	Bootstrap analysis (100 pseudoreplicates for ML, 10 random additions for each of 100 bootstrap pseudoreplicates for MP)	Validation of tree topology through bootstrap support
12	AFP mRNA sequences from various beetle species	ML	MEGA7	Bootstrap values (500 replications)	Validation of tree topology through bootstrap support	
Convergent evolution	63	The sequences of type II AFPs and related lectins were downloaded from the NCBI through PSI-BLAST searches using the herring AFP sequence as a query	Maximum likelihood	MUSCLE and PHYML	WAG model; bootstrap test with 100 replications	Comparison with known phylogenies; validation of tree topology robustness

Table 1 (continued)

Ref.	Data	Evolutionary models	Software	Parameters	Validation/additional analyses
81	Additional type I AFP sequences from sculpin ( <i>Myoxocephalus</i> spp.) and reference sequences from winter flounder, cunner, and snailfish obtained from GenBank	Convergent evolution (hypothesized based on sequence similarity and lack of common ancestry)	DNAMAN, EMBOSS suite (for sequence manipulations and codon usage analysis), BLAST (for database searches)	No explicit phylogenetic models were applied	Sequence alignments, dot matrix comparisons, codon usage analysis, BLAST searches against databases; comparison of coding and non-coding regions, lack of similarity in UTRs, and dramatic differences in Ala codon usage among species support convergent evolution
82	Genomic and transcriptomic sequences of cunner ( <i>Tautoglabrus adspersus</i> ), snailfish ( <i>Liparis</i> spp.), flounder, and sculpin obtained from NCBI databases; reference type I AFP sequences from previous studies	Convergent evolution of type I AFPs in four fish lineages (cunner, snailfish, flounder, sculpin)	BLAST, SnapGene Viewer, GeneWise, MEGA, AlphaFold2, PyMOL	BLAST settings (discontiguous megablast, BLOSUM45 matrix), phylogenetic tree construction parameters (JTT G + I model, 100 bootstrap replicates), codon usage statistics calculation	Sequence alignments, phylogenetic tree analysis, codon usage bias analysis, promoter element prediction, repetitive element identification, and modeling of AFP structures using AlphaFold2; comparison of gene loci, synteny, and sequence similarity to support the convergent evolution hypothesis

### 3.4 Genomic synteny

Genomic synteny is also commonly employed for studying the evolution of AFPs. For instance, Graham sequenced a smelt BAC clone containing the AFP gene and compared the syntenic regions in other fish genomes. They found that the AFP gene was absent in the corresponding regions of other species, supporting that there was a HGT event between smelt and herring. Moreover, the introns of the AFP gene in smelt and herring were highly conserved, but the introns in adjacent genes were highly diverged. This result further confirmed the HGT hypothesis.<sup>74</sup>

### 3.5 Others

Other methodologies such as dot matrix analyses and chromosomal FISH experiments are also highly prevalent and frequently employed technical approaches. For instance, digoxigenin was employed to label type III AFP genes in metaphase chromosomal preparations obtained from *L. dearborni*. Following visualization and image acquisition, an SAS gene probe was labeled under identical conditions. Consequently, the positional relationships between the SAS gene and type III AFP genes were elucidated.<sup>67</sup>

## 4. Escape from adaptive conflict

Escape from adaptive conflict (EAC) refers to a situation where an existing gene acquires a subfunctionalization besides its primary function, which can be subjected to the natural selective pressure. Therefore, an adaptive conflict

emerges between the new and old functions, constraining their further improvements.<sup>83,84</sup> Gene duplication can effectively resolve this conflict, allowing several copies to continue the original function, while others undertake selective changes, leading to subfunctionalization.<sup>83,85,86</sup> To date, several types of AFPs have evolved from functional unrelated genes and exhibit a clear evolutionary process of resolving adaptive conflicts.<sup>72,87,88</sup> Herein, the evolutionary processes of type III AFPs and Antarctic AFGPs are discussed, all of which evolved through the EAC process. In fact, EAC also participated in the evolutionary process of type II AFPs. But considering that the detailed EAC process of type II AFPs requires further investigation, and given its involvement in another evolutionary model of HGT, we introduced it in the third part.

### 4.1 Type III fish

Type III AFPs, with around 7 kDa, are small globular proteins.<sup>89</sup> Currently, they can be found in Zoarcoid families specifically within both *Zoarcidae* and *Anarhichadidae*, suggesting that they may have evolved from a monophyletic infraorder. To date, the emergence of type III AFPs has been traced back to a common ancestor, and they are believed to have originated from the duplication of the sialic acid synthase (SAS) gene.<sup>88</sup> In 2001, a paper from a public funded sequencing effort (International Human Genome Sequencing Consortium) revealed that the sequences of human SAS (BAA91818.1) are homologous to type III AFPs found in fish.<sup>88</sup>

Deng *et al.* constructed a bacterial artificial chromosome (BAC) library of the Antarctic eelpout *Lycodichthys dearborni* which contains both the SAS gene and type III AFP gene to explore the evolutionary process of type III AFPs from zoarcid SAS.<sup>90</sup> Initially, it was revealed that the SAS locus has two SAS homologues including SAS-a and SAS-b, separated by a chicken repeat-type retrotransposon (*LdCR1-3*) (Fig. 3A). SAS-a and SAS-b both have 6 exons and are similar to each other both in their coding sequences (92%) and intervening introns (67%), and they both show high identity to type III AFPs. However, while SAS-a and type III AFP exhibit distinct flanking regions, SAS-b shows a high degree of similarity to type III AFP in its 5' UTR and 5' flanking regions. Specifically, a 54-nucleotide sequence located upstream of the 5' UTR of SAS-b displays 64% identity to the signal peptide of type III AFPs. Furthermore, both the type III AFP locus and the SAS-b locus contain a partial CR1-3 retrotransposon (*LdCR1-3*). These findings suggest that type III AFP originated from SAS-b (Fig. 3B).

The localization of the SAS gene and type III AFP gene depicts that they are located on distinct metaphase chromosome pairs, both having only one locus (Fig. 3C and D). Moreover, the type III AFP locus is flanked by *Glud1b* and *Synuclein* genes at the N-terminal and *LIM domain binding 3b* and *Melanopsin* at the C-terminal, respectively. In contrast, the SAS gene is flanked by *CLTA* and *NCKX2* genes at its two ends, which is distinct from the flanking genes of type III AFP. Altogether, these results suggest that type III AFP was duplicated and translocated from the SAS-b gene. When SAS-b was transformed into the type III AFP gene, the majority of its E1 and E2–5 were lost. Subsequently, the 5' UTR, partial E1, I5, E6 and 3' UTR regions were recruited together and transformed into a novel protein of type III AFP.<sup>88</sup>

Based on the above-mentioned molecular process, Deng *et al.* have proposed the EAC evolutionary model of type III AFPs: initially, the ancestral SAS gene had a primary ability to catalyze the conversion of *N*-acetylmannosamine or Man-NAC-

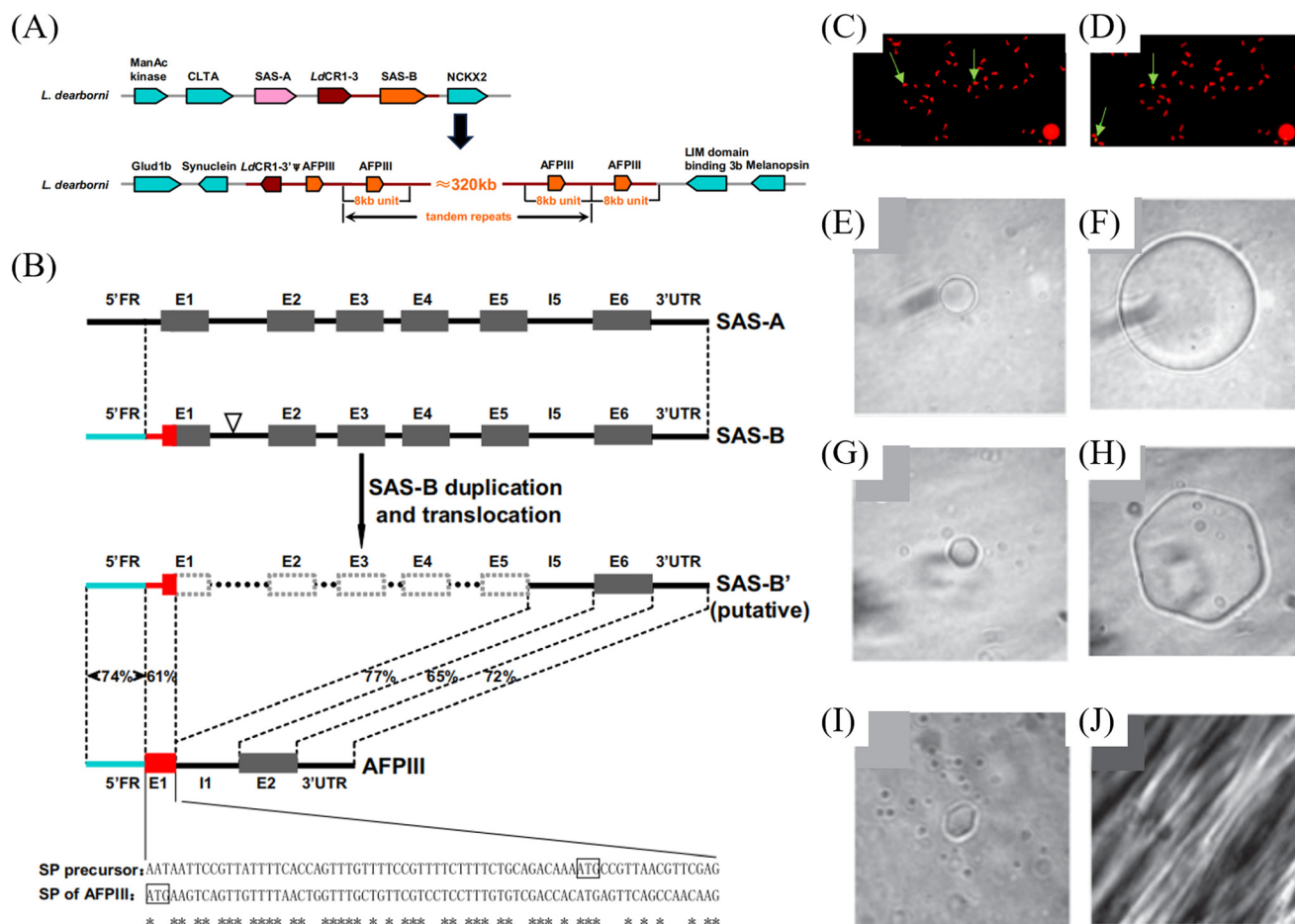


**Fig. 3** (A) The genomic organization of SAS and type III AFP loci in *L. dearborni*. (B) The molecular process of type III AFPs evolved from SAS-B. (C and D) The localization of *L. dearborni* SAS (A) and type III AFPs (B) by FISH experiments. The green arrows indicate the location. (E–J) Dynamic ice shaping ability of water (E and F), the recombinant *LdSAS-B* with 2 mg mL<sup>-1</sup> (G and H) and type III AFP of the eelpout (I and J). The ice crystal morphology was discoid in water (E) but was faceted in *LdSAS-B* (G) and type III AFP (I) solutions. When the temperature reached the equilibrium point of water, the ice was still discoid (F). In contrast, when the temperature was at a nonequilibrium freezing point, the ice displayed a hexagonal disk (H) or underwent an explosive growth (I). Reprinted with permission from ref. 88. Copyright (2010) *Proc. Natl. Acad. Sci. U. S. A.*

6-phosphate and phosphoenolpyruvate to sialic acids, along with a secondary and weaker ability to produce antifreeze simultaneously (Fig. 3E–H).<sup>91</sup> However, the antifreeze function became more prominent when the gene was subjected to strong selective pressure from late Cenozoic sea-level glaciation.<sup>92</sup> This led to a conflict between the two distinct functions due to their different substrate specificity and spatial distribution. Therefore, gene duplication became

necessary and the evolution of type III AFP was observed as a result of this functional conflict (Fig. 3I and J).<sup>88</sup>

#### 4.2 Antarctic AFGP

To investigate the origin of Antarctic AFGPs, Chen *et al.* searched the GenBank database and identified that the trypsinogen gene is homologous to Antarctic AFGPs.

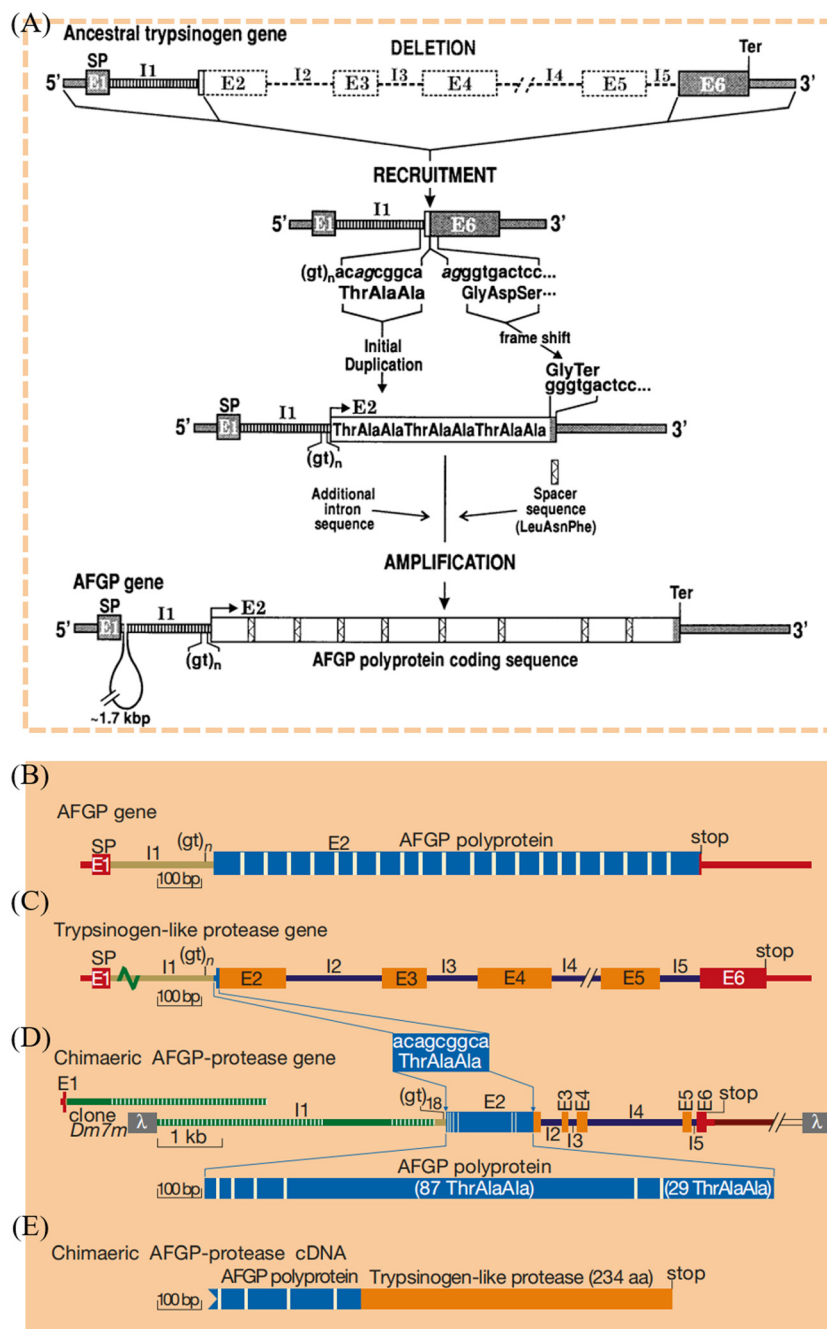


**Fig. 4** (A) Likely mechanism by which an ancestral trypsinogen gene was transformed into an AFGP gene. Reprinted with permission from ref. 72. Copyright (1997) *Proc. Natl. Acad. Sci. U. S. A.* (B) The structure of an Antarctic AFGP gene. (C) The structure of a trypsinogen-like protease gene. (D) The structure of a chimaeric AFGP-protase gene. (E) The structure of a chimaeric AFGP-protase cDNA. The AFGP coding sequences are colored in blue. The spacer and the signal peptide sequences are colored in pink. The trypsinogen-like protease coding sequences are colored in orange. Reprinted with permission from ref. 73. Copyright (1999) *Nature*.

Compared to the original trypsinogen, it was revealed that the 3' flanking sequence of Antarctic AFGPs was around 80% identical to the exon 6 (E6) of trypsinogen, revealing their close relationship. Therefore, it was inferred that Antarctic AFGPs originated from trypsinogen based on the above results. Analysis of the alignments of cDNAs and genes between Antarctic AFGPs and trypsinogen has revealed some remarkable similarities. Initially, the E1 region of Antarctic AFGP, which encompasses the 5' UTR and signal peptide, shows complete sequence identity to the corresponding part of the trypsinogen gene. Besides, the 3' UTR region of the AFGP gene starting from the penultimate codon is also identical to the E6 of the trypsinogen gene. Moreover, intron 1 (I1) of the AFGP gene exhibits 93% identity with the entire I1 of the trypsinogen gene.<sup>72</sup> Based on these findings, it was proposed that the evolutionary process of Antarctic AFGPs from the trypsinogen gene is as follows: the Antarctic AFGP was formed through the recruitment of E1, I1, several nucleotides of E2 including a 9-nt Thr-Ala-Ala coding element, E6 and 3' UTR of trypsinogen, whereas the rest of E2 through I5 was lacking. During evolution, the 9-nt Thr-Ala-Ala coding element underwent amplification, thus leading to a frameshift of the recruited E6 and the acquisition of a termination codon located behind a codon encoding Gly. In addition, a 1.7 kbp sequence was added into the I1 and a tripeptide of Leu/Phe-Ile/Asn-Phe acting as a spacer was adjoined to Thr-Ala-Ala repeats through preexisting sequence or recombination events. However, the deletion, amplification and recruitment events were not in the order given (Fig. 4A).<sup>72</sup>

Interestingly, Cheng *et al.* obtained a complete chimaeric gene (~11 kb) through screening the whole genomic library of a giant Antarctic toothfish *Dissostichus mawsoni* (Fig. 4D). This chimaeric gene contains six exons and five introns, displaying a significant similarity to trypsinogen-like protease genes (Fig. 4C–E). However, E2 in this chimaeric gene has a large 5' AFGP polyprotein-coding segment (Fig. 4B), which is thought to be the product of the amplification of the element of Thr-Ala-Ala.<sup>73</sup> The existence of this chimaeric gene indicated that the amplification of Thr-Ala-Ala tripeptides occurred before the deletion event, which is believed to be a more stable structure than the large deletion before the amplification event.<sup>72</sup> Moreover, the simultaneous existence of a chimaeric AFGP-protease gene and an incipient Thr-Ala-Ala element was found in the toothfish genome, further indicating that AFGP genes started out as a small part of the protease gene.<sup>73</sup> Under the selection towards freezing and expansion, they acquired the independence by shedding the substantial part of the protease sequences.<sup>73</sup> There is also a question regarding why trypsinogen is transformed into AFGPs under the selective pressure of cold temperatures. A possible explanation lies in the behavior of Antarctic notothenioids. When these fish search for food and take in seawater, ice crystals are inevitably ingested into their intestinal fluids. As a result, AFGPs and trypsinogen can reach the digestive

tract simultaneously, and the AFGPs can prevent the ice crystals from freezing.<sup>72</sup>

### 4.3 EAC-inspired design of antifreeze materials

As mentioned above, for instance, the recruitment of specific exons and introns from trypsinogen is followed by the amplification of a Thr-Ala-Ala tripeptide repeat, resulting in an AFGP protein capable of inhibiting ice recrystallization.<sup>72</sup> In other words, genes acquire antifreeze activity through duplication, accompanied by fine-tuning of gene sequences and structures. This enables the new gene to specifically bind to ice crystals, thereby regulating ice growth and recrystallization. This process represents the development and optimization of antifreeze molecules by nature through trial-and-error processes, providing guidelines for designing new types of antifreeze materials. Herein, we present several examples akin to this process.

In 2016, Liu *et al.* revealed that AFPs possess both an ice-binding face (IBF) and a non-ice-binding face (NIBF). The IBF can organize the water molecules into hexagonal ice-like structures through its unique arrangement of methyl and hydroxyl groups, thus promoting ice formation. In contrast, the NIBF disrupts the organization of ice-like structures with its irregular arrangement of hydrophobic/hydrophilic groups as well as the bulky hydrophobic groups and charged groups, thereby depressing the ice formation.<sup>93</sup> Inspired by this, Yang *et al.* developed an ice-controlling copolymer poly(SBMA-co-NIPAAm) (PSN) consisting of polar (sulfobetaine methacrylate) (SBMA) and nonpolar *N*-isopropylacrylamide (NIPAAm). Specifically, polar SBMA was utilized to simulate the IBF and nonpolar NIPAAm was employed to mimic the NIBF. They substituted the degradable protein-based amino acid chains with highly stable polymers while preserving the IBF and NIBF of AFPs, mirroring the evolutionary trajectory of EAC. As a result, PSN can bind to ice crystals and displays excellent IRI activity. When employed for cryopreservation, the cell survival rate of GLC-82 cells reached 97%.<sup>94</sup> Similarly, Tian *et al.* designed a poly(dimethylsiloxane-co-sulfobetaine methacrylate) (PDSB) copolymer, in which pristine polydimethylsiloxane (PDMS) was used to mimic the IBF of AFPs, while PSBMA mimicked the NIBF. This design retained the key functional properties of AFPs but replaced the amino acid chains with PDSB and PSBMA, respectively (Fig. 5A). Thus, the PDMS binds to the ice crystals and the PSBMA binds to the water molecules through the ionic solvation effects, thereby preventing them from freezing and effectively delaying icing from 7 s to 339 s.<sup>95</sup> In addition, Yu *et al.* designed several graphene oxide (GO) nanosheets that were functionalized with different kinds of charges. GO was employed to mimic the IBF while the varied charges served to modify the NIBF (Fig. 5A). Specifically, the zwitterionic GO nanosheets exhibited superior performance in anti-icing, demonstrating an impressive ice delay capability ranging from 40 s to 953 s.<sup>96</sup> These above AFP mimics were all developed by employing more stable and cost-effective

The process of developing antifreeze materials is similar to the EAC process.

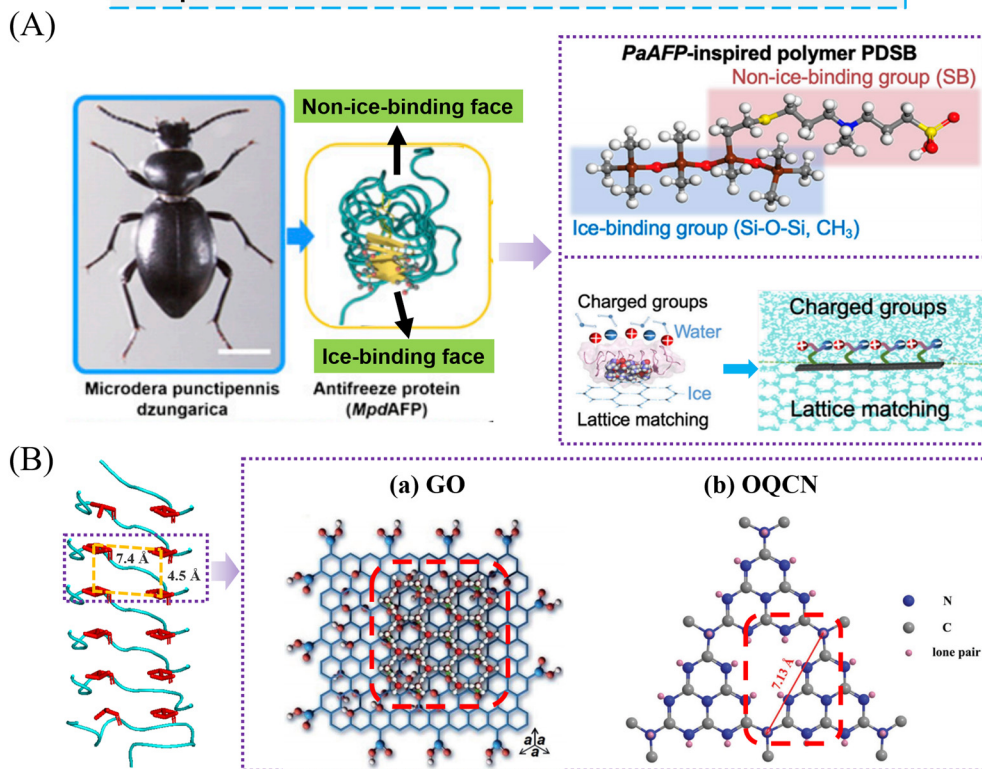


**Fig. 5** (A) The structure of AFPs, which possess both an IBF and a NIBF. The copolymer PDSB was developed based on this structure. Reprinted with permission from ref. 93, 95 and 96. Copyright (2016) NAS, (2023) AAAS, and (2025) ACS. (B) The structure of the ice-binding surfaces of *Tm*AFPs (PDB ID: 1EZG). (a) The schematic illustration of GO interacting with ice crystals. Reprinted with permission from ref. 34. Copyright (2017) Wiley. (b) The structure of OQCN. Reprinted with permission from ref. 35. Copyright (2017) Wiley.

polymers as their building blocks, rather than relying on specifically designed amino acid peptide chains. This process innovatively integrates the diverse advantages of the stability of polymers with the efficient functional models of AFPs, while simultaneously mitigating their drawbacks, akin to the evolutionary process of EAC. Thus, compared to natural AFPs, they possess the advantages of ease of acquisition, low cost, and structural stability as well as maintenance of the antifreeze activity.

Besides, as is well known, the ice-binding ability of natural AFPs is primarily attributed to their specific structures, whose side-chain O atoms on the ice-binding surfaces have a spacing of 7.4 Å wide and 4.6 Å long, matching the spacing of O atoms of basal and prism planes of ice.<sup>60,97–99</sup> Therefore, numerous mimics of AFPs have been proposed. During the design process, the structural characteristics were retained, yet these mimics lacked the component of the easily degradable amino acid chains, which was similar to the EAC process. For instance, the hydroxy groups of the repeated honeycomb hexagonal carbon rings of GO are arranged into a rectangular array with a width of 7.4 Å and a length of 4.3 Å, implying its ability to mimic AFPs in controlling ice growth and recrystallization (Fig. 5B-a). Geng *et al.* employed it to substitute AFPs for cryopreservation of horse sperms and the

motility was increased from 24.3% to 71.3%.<sup>34</sup> Besides, it has been revealed that the distance between two neighboring tertiary N atoms is 7.13 Å, matching with the primary prism plane of ice crystals (Fig. 5B-b).<sup>35</sup> In addition, Deller *et al.* employed nontoxic polyvinyl alcohol (PVA) to cryopreserve both sheep and human RBCs, which can mimic the IRI function of AFPs. It was revealed that only 0.1% PVA could significantly increase the cell recovery from 0 to 40%.<sup>22</sup> Moreover, a type of Zr-MOF was developed to mimic the structure of AFPs, coated with hydrogen groups on its surface, enabling it to precisely match ice crystals. When used as CPAs, it can also effectively improve the cell recovery of RBCs.<sup>100</sup> Thus, these AFP mimics present stability and ease of acquisition compared to natural AFPs.

In our view, the EAC-inspired design approach for antifreeze materials aims to create antifreeze molecules that retain the ice-binding functions of AFPs while eliminating undesirable aspects like the high immunogenicity and degradability of AFPs. This design approach aligns with the engineering strategies of function-oriented material design by providing a clear framework for optimizing material properties. The design methodology based on the EAC model incorporates techniques such as polymer functionalization, which integrate specific structural motifs responsible for ice binding.

## 5. *De novo* evolution

In contrast to EAC, *de novo* genes are not restricted by the adaptive conflict or antagonism between the new and the old functions. It has been revealed that *de novo* genes play a crucial role in enabling species to adapt to climate change and have been reported in diverse organisms such as animals and plants.<sup>101</sup> Among the AF(G)P families, AFGPs from Arctic codfish are considered as an exemplary case for *de novo* gene evolution.<sup>43</sup>

### 5.1 AFGPs from Arctic codfish

AFGPs in Arctic codfish comprise a family of polypeptides with discrete sizes ranging from 2.6 kDa to 34 kDa.<sup>102</sup> They

are highly conserved and generally made of approximately identical glycotriptide repeats of Thr-Ala/Pro-Ala (known as TAA) with a disaccharide of galactosyl-*N*-acetylgalactosamine linked to the threonine residues, similar to Antarctic AFGPs.<sup>103</sup>

Zhuang *et al.* revealed that the AFGPs found in Arctic codfish did not evolve from an ancestral functional protein. This conclusion was based on the observation that there were no meaningful homologs between the AFGP genes of Arctic codfish and the genes/genome sequences available in databases. This finding suggested that the AFGP genes in Arctic codfish may originate from noncoding sequences because the lack of homology can be attributed to rapid mutation or recombination that occurred during evolution.

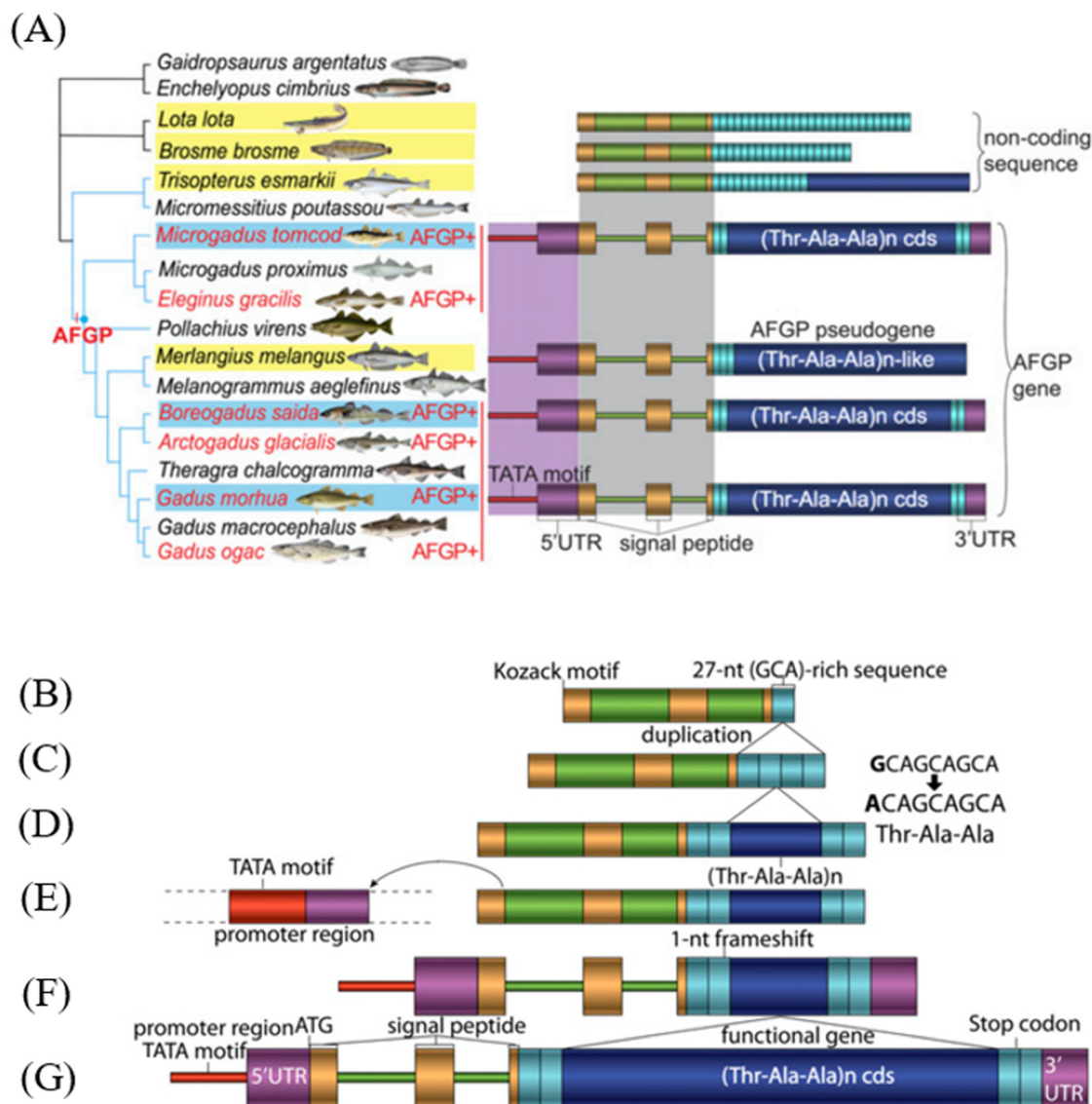


**Fig. 6** (A) The phylogenetic tree of codfish AFGPs including both AFGP-coding (blue) and AFGP-lacking organisms (yellow). The genomic structures are on the right of the phylogenetic tree. (B–G) Evolutionary process of the codfish AFGPs. Gray and purple shaded areas indicate the homologous regions of the signal peptide sequence and *cis* transcriptional components, respectively. Light blue indicates the 27-nt duplicates. Dark blue indicates the 9-nt of Thr-Ala-Ala repeats. Purple indicates the 5' or 3' UTR region. Red indicates the TATA motif. Reprinted with permission from ref. 43. Copyright (1997) *Proc. Natl. Acad. Sci. U. S. A.*

Such genetic alterations are more prevalent in non-coding regions due to their inherent flexibility and variability.<sup>43</sup>

Subsequently, they constructed phylogenetic trees using the genomic libraries of several northern cod organisms, which included both AFGP-producing and AFGP-lacking variants, to uncover the evolutionary relationships among them. As shown in Fig. 6A, AFGP-bearing *Boreogadus saida* and *Gadus morhua* were grouped within one subclade, while *Microgadus tomcod* formed another subclade. The AFGP-lacking *Merlangius merlangus* shared a common ancestor with *B. saida* and *G. morhua*. Besides, the AFGP-lacking *Trisopterus esmarkii* is basal to the two AFGP-bearing subclades, and *Brosme brosme* and *Lota lota* were considered as ancestral proxies prior to the appearance of AFGPs.<sup>43</sup> To trace the origin of the AFGP genotype, they conducted a comparative analysis to identify the differences between them.<sup>43</sup>

Among all the components of AFGPs in Arctic codfish, the main constituents are TAA tripeptide repeats in the coding regions, a TATA box response for the function of transcriptional activation and a signal peptide. For TAA repeats, it was revealed that they originated from a pair of 27-nt GCA-rich duplicates. Notably, within these conserved 27-nt GCA-rich duplicates, there are many 9-nt elements of Pro/Ala-Ala-Ala. When a 1-nt substitution (C → A or G → A) occurs at the first position of the 9-nt element, a tripeptide unit of Thr-Ala-Ala emerges. This 9-nt element then undergoes expansion and arrives at tandem duplications in AFGP-coding sequences (Fig. 6B and C). Subsequently, as shown in Fig. 6D, the 27-nt duplicates are spread apart to flanking positions. As depicted, aside from AFGP-coding sequences, the homolog of 27-nt duplicates also exists in other AFGP-lacking sequences (Fig. 6A). Interestingly, additional 1-nt mutations occur throughout the whole sequences, thereby increasing the sequence complexity and preventing the expansion or contraction of the repeat by homologous recombination.<sup>43</sup>

For the TATA box, Zhuang *et al.* compared the upstream regions of both AFGP-coding and AFGP-lacking organisms. It was observed that the upstream regions of all AFGP-coding organisms share high similarities. In contrast, AFGP-lacking organisms show significant differences when compared to AFGP-coding organisms, yet they display a high level of similarity among themselves.<sup>43</sup> Based on the above mentioned, it was deduced that a stochastic translocation occurred, leading the most common ancestor of AFGP-coding organisms to acquire a TATA box and subsequently gain transcriptional ability.<sup>43</sup>

Moreover, as Arctic codfish AFGPs generally function at circulating fluids, a signal peptide was acquired. Through the alignment among the sequences of *B. saida* AFGP genes, *M. merlangus* AFGP pseudogenes and *T. esmarkii* noncoding AFGP homologs, Zhuang *et al.* deduced that the signal peptide originated from the 27-nt duplicate II upstream of the 9-nt tripeptide repeats. Specifically, with a 1-nt deletion of “T”, a reading frameshift occurred, and the upstream sequence could supply as a signal peptide being linked to the

tripeptide repeats, thus forming a single open reading frame (Fig. 6F).<sup>43</sup> The expression and secretion of a novel AFP become possible. This novel AFP consists of three exons and two introns. The former two exons and the first 2nts of E3 encode the signal peptide, while the rest of the E3 encodes a short pro-peptide and the long AFGP polyprotein (Fig. 6G). Therefore, a functional AFGP gene was obtained in Arctic codfish and this novel gene endowed Arctic codfish with the ability to survive in chilly environments.<sup>43</sup> Alternatively, a highly diverged homolog might exist but remain undetected—future genome assemblies could test this.

## 5.2 *De novo* evolutionary model-inspired design of antifreeze materials

As was discussed above, the *de novo* evolution of the AFGP gene in northern gadids emerged from noncoding sequences through the interplay of mutation and natural selection, independent of pre-existing genes. During this evolutionary process, all necessary regulatory elements—including the TAA tripeptide repeats, a TATA box, and a signal peptide—were co-opted, culminating in the formation of a novel antifreeze molecule.<sup>43</sup> Analogously, material design methodologies inspired by the *de novo* evolutionary model also necessitate the integration of all essential “regulatory elements” to create novel antifreeze materials.

Herein, we have identified several instances that mirror the *de novo* evolutionary model. For instance, Gao *et al.* developed a dynamic membrane-active glycopeptide named PMB. This glycopeptide was synthesized by incorporating several “regulatory elements”: a cationic polymer scaffold  $\epsilon$ -poly(L-lysine) ( $\epsilon$ -PL), maltotriose, and *p*-benzyl alcohol. Thus, this glycopeptide PMB can facilitate trehalose entry into cell membranes by perturbing the phospholipid bilayer with *p*-benzyl alcohol along with stabilizing the membrane with maltotriose. As a result, the cell recovery can reach >95% when employing PMB as a cryoprotectant (Fig. 7A).<sup>104</sup> In our opinion, the process of constituting the glycopeptide PMB is much similar to the process of *de novo* evolution. In this process, the “regulatory elements” intended to promote the entrance of trehalose into cells are combined and function synergistically. Similarly, Guo *et al.* successfully synthesized an amphiphilic material PVP-PDMS-PVP by integrating essential “regulatory elements”: polyvinylpyrrolidone (PVP) with strong ability to inhibit ice nucleation and polydimethylsiloxane (PDMS) with low surface energy. When this amphiphilic material is employed as an anti-icing coating, it exhibits a 34-fold increase in freezing delay time compared to control steel, accompanied by an ice adhesion strength of about 18 kPa (Fig. 7B).<sup>105</sup> Moreover, Chen *et al.* also synthesized a polymer named PVA-PFA-PDMS. The “regulatory elements” incorporated include PDMS, PFA (with lower surface energy than PDMS) and PDMS, respectively. When used as an anti-icing coating, it also demonstrates a reduced ice adhesion strength (~17.7 kPa) (Fig. 7C).<sup>106</sup> The cases we have reviewed here serve as

The process of developing antifreeze materials is similar to the *de novo* evolution process

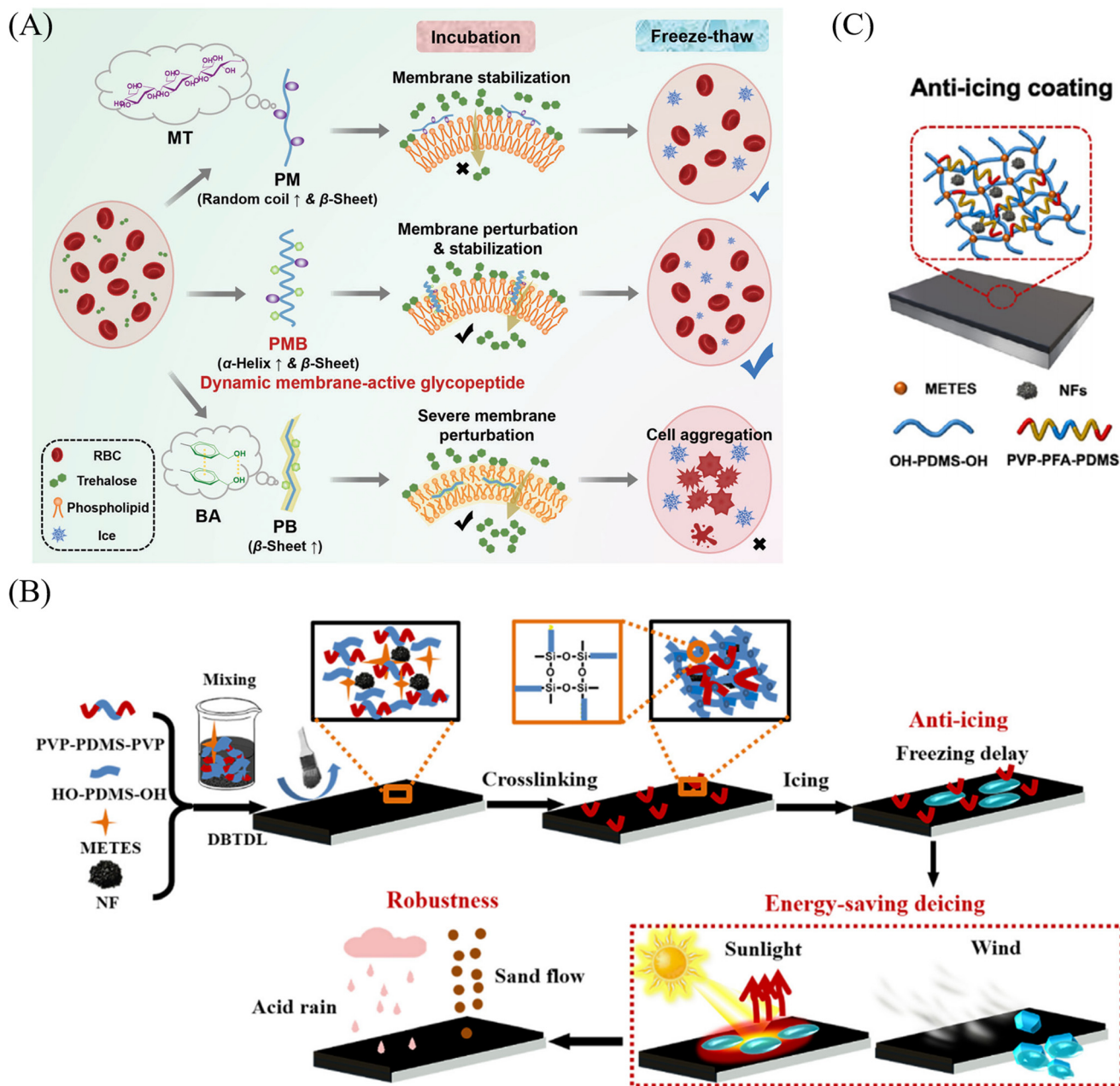


**Fig. 7** (A) The schematic illustration of a dynamic membrane-active glycopeptide named as PL-g-(MT/BA) (PMB). Reprinted with permission from ref. 104. Copyright (2023) Wiley. (B) The schematic illustration of an anti-icing coating made of the polymer PVP-PDMS-PVP with nanocarbon fiber (NF). Reprinted with permission from ref. 105. Copyright (2020) Elsevier. (C) The schematic illustration of an anti-icing coating made of the polymer PVP-PFA-PDMS consisting of PVP, PFA and PDMS, respectively. Reprinted with permission from ref. 106. Copyright (2022) Elsevier.

guidelines for designing antifreeze materials from scratch in the future.

In our opinion, this *de novo* evolutionary model-inspired designing method can be explicitly mapped onto an integrated engineering strategy. Within this mapping process, various useful “regulatory elements” with an appropriate dosage and location have been integrated. As a result, new

and useful antifreeze materials can be generated more efficiently and effectively.

## 6. Horizontal gene transfer

Horizontal gene transfer (HGT), also known as “the non-genealogical transmission of a genetic material from one

organism to another”, is distinct from the vertical transferring of genetic materials between generations.<sup>107,108</sup>

In most cases, the confirmation of HGT events relies on the differences in the topology of phylogenetic trees between the gene of interest and the phylogeny of an accepted group of organisms.<sup>109</sup> In the sea, the solid ice can serve as a stabilizing substrate for DNA attachment, thereby increasing the DNA concentrations 13 times higher than under-ice ocean.<sup>110–112</sup> It is assumed that HGT events occurred frequently during the AF(G)P evolutionary process because AF(G)P-produced organisms are generally inhabiting in sea-ice surroundings, which is considered as a “hot pot” for HGT.<sup>112</sup> Herein, the evolution process of type II AFPs, DUF3494 AFP family members and insect AFPs are introduced, which are representative of the HGT process.

## 6.1 Type II fish

In 1992, Ewart *et al.* successfully cloned the type II AFPs from the liver of rainbow smelt (*Osmerus mordax*) and demonstrated their homology to a family of calcium-dependent lectins (C-type lectins) by BLAST alignment.<sup>113</sup> In 2008, Graham *et al.* used Atlantic herring (*Clupea harengus*), rainbow smelt and sea raven (*Hemitripterus americanus*) type II AFPs as queries to explore their close sequences. As a result, they also found that the closest homologs were fish lectin-like proteins, whose sequence identity was around 40%.<sup>114</sup> Subsequently, an increasing amount of evidence has demonstrated that type II AFPs and C-type lectins have homology and share a similar structural fold and function.<sup>53</sup> Functionally speaking, C-type lectins can bind to the noncarbohydrate ligand ice.<sup>87,113,115</sup> This binding ability is

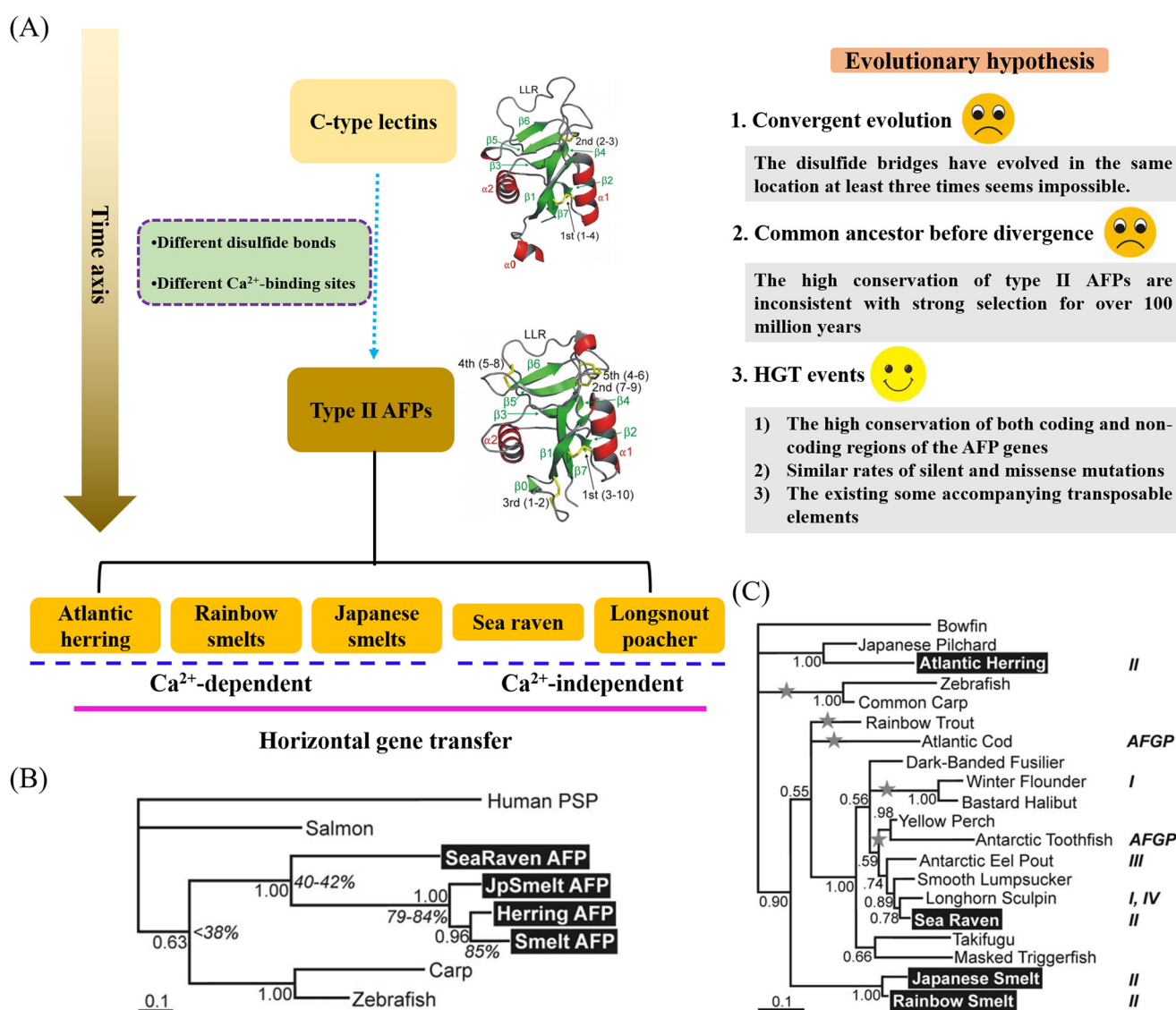


**Fig. 8** The evolutionary process of type II AFPs. (A) The structure of type II AFPs and C-type lectins. (B and C) The phylogenetic trees constructed from the AFP and related lectin sequences (B) as well as the ribosomal 16S RNA sequences (C). Reprinted with permission from ref. 114. Copyright (2008) *PLoS One*.

particularly significant as it highlights a functional aspect shared with AFPs. From a structural perspective, disulfide bonds and the majority of the conserved residues that form the tertiary structure of C-type lectins are also found in smelt type II AFPs.<sup>113</sup> This structural similarity further cements the connection between the two, suggesting that their shared structural elements may underlie the observed functional similarities. However, there exist primarily two differences between type II AFPs and C-type lectins. First, the number of disulfide bonds is different. Distinctly from C-type lectins containing 2 or 3 disulfide bonds,<sup>115,116</sup> type II AFPs generally have 5 disulfide bonds (Fig. 8A), but when the additional 2 disulfide bonds appeared is not clear. Second, their Ca<sup>2+</sup>-binding sites are different. Incidentally, type II AFPs secreted by rainbow smelt, Japanese smelt (*Hypomesus nipponensis*) and Atlantic herring are Ca<sup>2+</sup>-dependent, while type II AFPs from sea raven and longsnout poacher (*Brachyopsis rostratus*) are not (Fig. 8A).<sup>87,114</sup> By the way, it has been revealed that fish skin mucus lectins have two Ca<sup>2+</sup>-binding sites while only one Ca<sup>2+</sup>-binding site is maintained in Ca<sup>2+</sup>-dependent type II AFPs.<sup>87</sup>

There are mainly five species including closely related and distantly related fish producing type II AFPs of around 14–24 kDa,<sup>87,114,117,118</sup> which are Atlantic herring, rainbow smelts, Japanese smelts, sea raven and longsnout poacher.<sup>119,120</sup> These organisms belong to *Teleostei*, which can be divided into four major monophyletic taxa including Elopomorpha, Osteoglossomorpha, Ostarioclupeomorpha and Euteleosteomorpha. Among them, Atlantic herring belongs to Ostarioclupeomorpha and rainbow smelts, Japanese smelts, sea raven and longsnout poacher are members of Euteleosteomorpha.<sup>75</sup> Regarding the origin of type II AFPs in five species from fish skin mucus lectins, there are three hypotheses. The first hypothesis has been proposed: the convergent evolution (Fig. 8A). However, this hypothesis suggests that the disulfide bridges have evolved independently in the same location at least three times, which appears unlikely.<sup>65</sup> This result suggests that convergent evolution is not true between type II AFPs and C-type lectins in the five species. The second hypothesis is that skin mucus lectins and type II AFPs share a common ancestor. Liu *et al.* constructed phylogenetic trees employing different kinds of type II AFPs and fish skin mucus lectins. As a result, type II AFPs shared a common branch with mannose or galactose-binding lectins. Moreover, these type II AFPs produced by distinct species are far more similar to each other than to other lectins, indicating their closer relationships. Based on the above results, Liu *et al.* proposed that type II AFPs originated from the duplication and subsequent subfunctionalization of the same ancestor teleost fish lectin, prior to the differentiation of the ancestral Clupeocephala into the Ostarioclupeomorpha and Euteleosteomorpha groups.<sup>87</sup> However, Graham *et al.* raised an objection to the common origin hypothesis. First, they revealed that the introns and exons of type II AFPs (the identity >85%) derived from distantly related organisms were highly conserved. Their

similarity extends to DNA sequences, whose identity was up to 97%. However, it was stated that Ostarioclupeomorpha and Euteleosteomorpha differentiated over 100 million years ago, which was inconsistent with their high conservation.<sup>114,121</sup> Second, distinct type II AFPs exhibit a low silent mutation rate. Notably, the ratios of the missense mutations to silent mutations ( $d_N/d_S$ ) were inversely proportional to the protein identity. For instance, the  $d_N/d_S$  ratios of 19 out of 20 genes that possess orthologs in both herring and smelt approximated a straight line, but type II AFPs were an exception.<sup>114</sup> The  $d_N/d_S$  of type II AFPs was approximately 1.0, significantly higher than that of other genes that have undergone strong natural selection in such a long time.<sup>114</sup> They constructed phylogenetic trees based on ribosomal 16S sequences and type II AFP sequences separately and compared them (Fig. 8B and C). The results depicted that the topology of the two phylogenetic trees was distinctly different from each other, indicating that HGT events occurred among type II AFPs (Fig. 8B and C).<sup>114</sup> Thus, they proposed that HGT events occurred among the type II AFPs, which contradicted Liu's viewpoint. In their opinion, the HGT hypothesis provides an explanation for why type II AFPs from different organisms are highly conserved; specifically, this suggests that there has not been sufficient time for mutations to accumulate in type II AFPs across these diverse organisms.

Research further shows that smelt AFPs were laterally transferred from herring AFPs.<sup>121</sup> The reasons are as follows: first, Southern blotting, qPCR and polymorphism results all depicted that there was a dearth of polymorphism in smelt AFPs but not in herring AFPs. Southern blotting results revealed that multiple bands were observed when amplification of herring AFP genes was performed using primers that targeted a conserved region. In contrast, there was only a single band of smelt AFP samples, indicating that it was a single-copy gene.<sup>114</sup> qPCR results also revealed that smelt AFPs just contain a single copy.<sup>121</sup> In addition, it was found that there were 31 polymorphic sites (5%) for herring AFPs while only one for smelt AFPs, consistent with the qPCR results. These results indicated that smelt AFPs have had little time to diverge.<sup>121</sup> Second, as previously reported, most types of AFPs including herring AFPs belong to multigene families, thus playing a more efficient role in cold resistance. In contrast, smelt AFPs are unique in that they serve as an adjunct to an already effective antifreeze strategy, rather than a necessary lifeline in desperate times.<sup>65,122–124</sup> Third, some accompanying transposable elements also support that the type II AFPs were transferred from herring to smelt.<sup>125</sup> Sorhannus raised an opposite using the phylogenetic analysis. They proposed that the transfer direction was from *O. mordax* to *C. harengus*. Aside from that, they also indicated two other HGT events: from *B. rostratus*–*H. americanus* to *H. nipponensis*–*O. mordax*, and from *B. rostratus*–*H. americanus*–*S. chuatsi*–*P. flavescens* to *P. flavescens*, respectively.<sup>117</sup> However, the transmission relationships among these five type II AFPs still require further research to be supplemented in the future.

## 6.2 DUF3494 AFP family

The members of the DUF3494 protein family refer to a series of proteins that contain a domain of unknown function (DUF) 3494, displaying a length of approximately 190 residues. They have been revealed to bind to ice crystals and control the ice growth and recrystallization, thus being regarded as AFPs.<sup>49</sup> DUF3494 family members can be found in various kingdoms of life including fungi, bacteria and microalgae.<sup>126–132</sup> These proteins typically share a similar 3D structure characterized by a discontinuous  $\beta$ -solenoid structure. The  $\beta$ -solenoid displays a triangular cross-section constituted by three  $\beta$ -sheets (designated as faces a, b and c) and an  $\alpha$ -helix along the a-face.<sup>133</sup> However, there are also some differences about their structures. To date, DUF3494 family members can be divided into three groups. The former two groups contain a “capping region” at the N-terminal top, resulting in higher antifreeze activities, while the third does not have, resulting in a lower antifreeze activity. Furthermore, the first group members contain a large cap but lack disulphide bonds while the second group members contain a large cap held by a disulphide bond (Fig. 9A). As for the functional domain, 68% DUF3494 proteins comprise a single domain, while the rest of them contain more than one functional domain (Fig. 9B). For example, IBPv derived from *Flavobacteriaceae* strain 3519-10 contains two consecutive DUF3494 domains connected by a 17-aa linker (Fig. 9B).<sup>134,135</sup> Such a complex tertiary structure of the DUF3494 domain is hardly evolved from diverse progenitors separately, and is considered because of HGT events.

Up to now, there have been numerous confirmed instances of the DUF3494 protein family being transferred *via* HGT from various organisms. For instance, Sorhan *et al.* constructed phylogenetic trees using SSU rRNA sequences and AFP/antifreeze-like protein (AFLP) sequences from the diatom genus *Fragilariopsis* organisms separately. Results depicted that there were several conflicts between the topological structures of the SSU rRNA and AFP trees. These results suggested that at least four instances of HGT events have occurred, leading to the transfer of AFPs to ice-living diatoms (Fig. 9C). Among them, two events occurred within eukaryotes (from the diatom *Chaetoceros neogracile* to the copepod *Stephos longipes* and from a basidiomycete clade to the diatom *Fragilariopsis* lineage), while the remaining two transfers were from an ascomycete lineage to the proteobacterium *Stigmatella aurantiaca* and from the proteobacterium *Polaribacter irgensii* to the ancestor of a group of 4 proteobacterium species.<sup>75</sup> Moreover, they also revealed that once obtained from the basidiomycetes (one of the 4 HGT events), the AFPs of the *Fragilariopsis* lineage further underwent extremely rapid evolution within a short period of time. These results indicated that the AFPs within an organism generally underwent independent evolution, not solely relying on HGT events.<sup>75</sup> To explore the intraspecific diversity of AFPs within *Fragilariopsis cylindrus* and

*Fragilariopsis curta*, Bayer-Giraldi *et al.* initially recognized 111 gene sequences for *Fragilariopsis cylindrus* and 102 gene sequences for *Fragilariopsis curta*.<sup>76</sup> Subsequently, they constructed a phylogenetic tree using all AFP sequences discovered in the *Fragilariopsis* lineage and their putative homologues.<sup>76</sup> The tree depicted that diatom AFPs were divided into two clades. *Fragilariopsis* AFPs were closely related to fungal and bacterial sequences, while the AFPs from *Navicula glaciei* and *Chaetoceros neogracile* were more associated with Archaea, indicating that these diatoms acquired their AFPs from different ancestors.<sup>76</sup> Uhlig *et al.* constructed phylogenetic trees to explore the diversity of DUF3494 proteins in Arctic and Antarctic sea-ice microbial environments.<sup>77</sup> The tree demonstrated that 89% proteins were grouped into two clades including “diatom” and “microalgae and copepod” clades. Most of the Arctic samples were associated with “diatom” while most of the Antarctic samples belonged to “microalgae and copepod”. They depicted that this observation was attributed to the geographic isolation between the two polar regions. Moreover, it was revealed that two HGT events occurred within their respective clades and one HGT event occurred between fungi and diatoms.<sup>77</sup>

It is speculated that HGT events are most commonly observed among members of the same taxonomic groups, such as prokaryotes, eukaryotes, and protists.<sup>8,136</sup> The transfers between eukaryotes and prokaryotes are undesirable because of the following reasons: first, eukaryote genes contain introns, which are absent in prokaryotes.<sup>137</sup> Second, the gene transfer in prokaryotes relies on the conjugation/transduction processes, which are not suitable for gene transfer from eukaryotes to prokaryotes attributed to their different expression regulatory mechanisms.<sup>137</sup> However, there have also been several rare reports of HGT events occurring between eukaryotes and prokaryotes.<sup>136</sup> For example, Raymond sequenced the AFP genes from *Chloromonas brevispina* and discovered that this organism possesses over 20 DUF3494 AFP isoforms. These isoforms exhibited a stronger association with fungal and bacterial AFPs compared to other algal AFPs, especially those from closely related species like *C. raudensis*.<sup>78</sup> These results suggested that the AFPs in *C. brevispina* were obtained through a HGT event from other AFP-producing microorganisms such as bacteria and fungi.<sup>78</sup> Besides, they identified an AFP in a diatom that inhabits the bottom layer of Antarctic Sea ice. This AFP shared 47% sequence similarity with a highly freeze-tolerant bacterium residing in the same layer and lacking introns, suggesting that a HGT event may have occurred between them.<sup>66</sup> To date, there are mainly two phyla of fungi, which are *Ascomycota* and *Basidiomycota*. In *Ascomycota*, *Antarctomyces psychrotrophicus* is the sole ascomycete known to produce AFPs (AnpAFP).<sup>136</sup> Arai *et al.* constructed cDNA libraries of *A. psychrotrophicus* and identified 3 candidate sequences of AnpAFP, which were designated as AnpIBP1a, AnpIBP1b and AnpIBP2, respectively.<sup>136</sup> These AnpAFP were found to be homologous

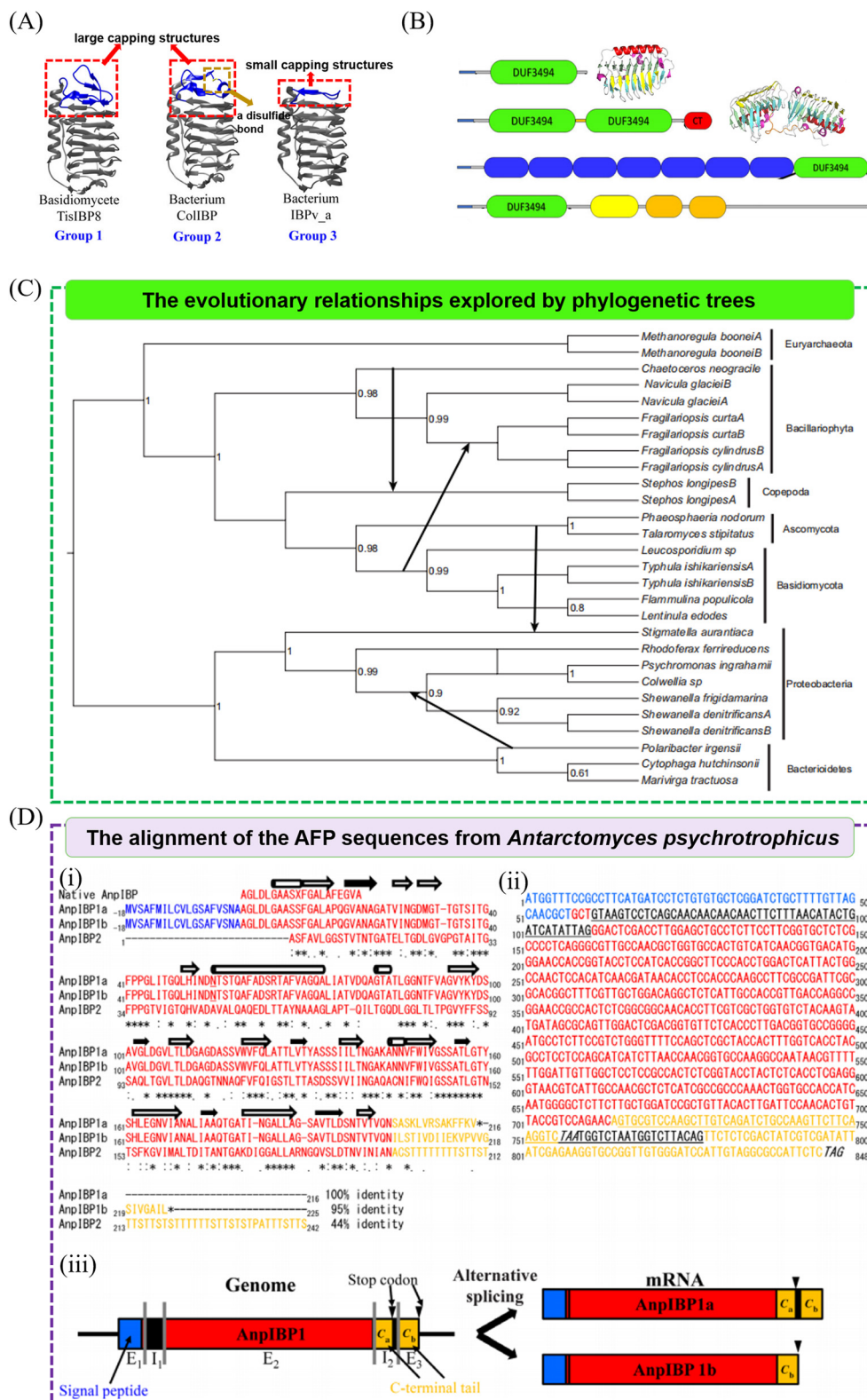


**Fig. 9** (A) Three kinds of DUF3494 family members. Group 1 depicts the protein with a capping region containing disulfide bonds. Group 2 depicts the protein with a capping region lacking disulfide bonds. Group 3 depicts the protein without a capping region. Reprinted with permission from ref. 136. Copyright (2019) Wiley. (B) Schematic diagram of the proteins containing DUF3494 domains. Reprinted with permission from ref. 49. Copyright (2019) Wiley. (C) The phylogenetic tree is constructed using SSU rRNA sequences. Four HGT events are labeled in the tree and the arrows depict the direction of gene transfer. Reprinted with permission from ref. 75. Copyright (2011) Sage Journal. (D) Schematic diagram of the genome structure and mature mRNA of AnpIBP. (i) The sequence alignment of the two isoforms of AnpIBP. (ii) The full-length AnpIBP1 gene in the genome. (iii) The genome structure and corresponding mature mRNA isoform structures of AnpIBP. C<sub>a</sub> and C<sub>b</sub> depict the C-terminal structure of AnpIBP1. Dotted lines depict the cleavage site. The blue color indicates the signal peptide, the black color represents the untranslated region, the red color corresponds to the DUF3494 region, and the yellow color signifies the C-terminal segment, respectively. Reprinted with permission from ref. 136. Copyright (2019) Wiley.

to DUF3494 family members through BLAST search identification. Among these three AFP sequences, the former two were almost identical to each other except their C-terminals, while they shared only 44% identity compared with the third sequence.<sup>136</sup> Besides, it was revealed that *AnpIBP2* in the genome does not contain an intron, whereas the *AnpIBP1b* gene has two introns. The second intron of *AnpIBP1b* is located at the end of the AFP domain. Alternative splicing of intron 2 results in the generation of *AnpIBP1a* and *AnpIBP1b* from one *AnpIBP* gene (Fig. 9D).<sup>136</sup> *AnpIBP1* and *AnpIBP2* were thought to be horizontally transferred from different bacteria separately, rather than a basidiomycete that has a closer relationship for the following three reasons: first, when their sequences were blasted by Protein Blast searches, it was revealed that their related sequences mostly belong to DUF3494 sequences from ascomycetes and bacteria. Moreover, the sequences most analogous to *AnpIBP1* were a putative IBP from an ascomycete *Zymoseptoria tritici* (58% and 66%), while the sequence displaying high similarity to *AnpIBP2* was a putative IBP from a planctomycete *Paludisphaera borealis* (72% and 76%).<sup>136</sup> The above cases indicated that the distribution of the DUF3494 protein family across different species serves as a typical example of HGT events.

### 6.3 Insect AFPs

**6.3.1 *TmAFP* and its homologues.** Most insect AFPs present repetitive motifs in both sequences and structures. Among them, *Tenebrio molitor* AFP (*TmAFP*) and *Choristoneura fumiferana* AFP (*CfAFP*) both display TH values of over 5 °C, presenting higher TH activities than most other AFPs. Their ice-binding surfaces are all constituted by TCT motifs, but it is depicted that they have distinct origins because: 1) their helix coils are in the opposite directions and they have different disulfide-bonding patterns, albeit they both contain  $\beta$ -helical structures. 2) Their primary sequences are different, in which *TmAFP* has a 12-residue repetitive motif of “TCTxSxxCxxAx” while *CfAFP* comprises a series of 15-residue repeats of “TCTxxxxxxxxxx”.<sup>138,139</sup>

It has been revealed that *TmAFP*s have undergone a positive Darwinian selection as the rate of nonsynonymous nucleotide substitution was much lower than that of synonymous substitution.<sup>80,140</sup> Besides, it has been depicted that *TmAFP* is homologous to *Dendroides canadensis*, *Microdera dzhungarica punctipennis*, *Anatolica polita*, *Dorcus hopei binodulosus* and *Dorcus rectus* AFPs because they all contain the 12-residue repetitive motif of TCTxSxNCxxAx.<sup>12,141–144</sup> Graham *et al.* collected 27 *TmAFP* isoforms and 11 *Dendroides canadensis* AFP (*DcAFP*) isoforms and both the cDNA and protein sequences of these isoforms were aligned.<sup>80</sup> As a result, the average identity was 67%, ranging from 55% to 88%, revealing that *TmAFP* and *DcAFP* were homologous. Graham *et al.* constructed a phylogenetic tree to reveal the relationship between *TmAFP*s and *DcAFP*s (Fig. 10A); the results depicted that they were divided into

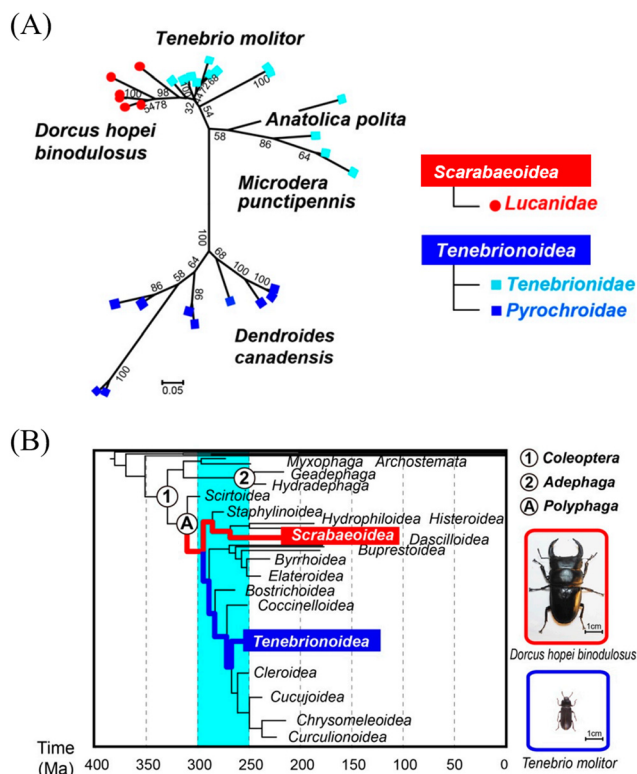


**Fig. 10** (A) The phylogenetic tree constructed using AFP mRNA sequences depicts the relationship among beetles. (B) The phylogenetic tree constructed using beetle superfamilies depicts the relationship among beetles. Reprinted with permission from ref. 12. Copyright (2021) Wiley.

two clades, albeit they were homologous (Fig. 10A). This was because of convergent evolution and the natural processes of birth and death within each species after they diverged.<sup>145</sup> Another striking feature of this tree was that there were much greater distances among *D. canadensis* isoforms than those among *TmAFP*s with mean *p*-distances of 0.22 and 0.094, respectively (Fig. 10A). This phenomenon was attributed to the variability of the third codon positions, which were 58% and 74% for *TmAFP*s and *DcAFP*s, respectively.<sup>145</sup> Generally, these results indicated that *T. molitor* has undergone climate change more recently and rapidly. In addition, it was found that the GC content was lower in both *TmAFP*s and *DcAFP*s at the third codon position, which was a specific phenomenon distinct from other genes in these two beetles.<sup>80</sup> As the GC content of functional RNAs has been reported to be negatively related to decreasing temperatures, it was postulated that the lower GC content may facilitate the transcription and translation at lower temperatures.<sup>80</sup> Aral *et al.* found that there were at least 6 isoforms of *Dorcus hopei binodulosus* AFPs (*DhbAFP*s), which contain the repetitive motifs of “TCTxSxNCxxAx” similar to *TmAFP*s. Furthermore, the first 28 residues of all *DhbAFP*s are termed as the signal peptides, also similar to *TmAFP*s. Blast search results indicated that the DNA similarity of *DhbAFP*s was around 82% and 67% compared to *TmAFP*s and *DcAFP*s, respectively.

In addition, the similarity of 5' and 3' UTR regions is 80–85% between *DhbAFP* and *TmAfp* genomes, indicating that they are homologous.<sup>12</sup> In addition to *DhbAFPs*, it has been discovered that *DrrAFPs* (*Dorcus rectus rectus* AFPs) possess the same repetitive motifs as those observed in *DhbAFPs*.<sup>12</sup> Arai *et al.* constructed phylogenetic trees to explore the evolutionary relationships among these beetle AFPs. As shown in Fig. 10B, it was depicted that *DhbAFPs* appeared the closest to *TmAfp*s. As *T. molitor*, *D. canadensis*, *A. polita*, and *M. punctipennis* belong to *Tenebrionoidea* whereas *D. h. binodulosus* and *D. r. rectus* fall into *Scarabaeoidea*, which have been branched off for an ultimately long divergence period of 250–300 million years, it was assumed that HGT events have occurred among these beetles due to the significant identity of DNA sequences of their AFPs.<sup>12</sup> However, the progenitor of these kinds of hyperactive AFPs in beetles is still waiting for further investigation.

**6.3.2 HhAFP and its homologues.** *Hypogastrura harveyi* AFPs (*HhAFPs*) primarily consist of two isoforms including a smaller one (6.5 kDa) and a larger one (15.7 kDa). The crystal structure of the smaller isoform comprises six helices, thus forming two layers. One layer is flat and hydrophobic, exhibiting ice-binding activity, while the other is rougher and hydrophilic.<sup>146</sup> The distinguishing feature of the primary sequence in this type of AFP is the abundance of Gly-X1-X2 motifs, where X1 frequently represents Gly.<sup>147</sup> In contrast, the large isoform is predicted to have a similar structure but with 13 helices.<sup>148</sup>

The springtail of *Megaphorura arctica* Tullberg 1876 is generally found in fields where the temperature can reach –20 °C in their winter time.<sup>149</sup> To investigate the antifreeze mechanism of *M. arctica*, Graham *et al.* extracted and purified AFPs from its crude homogenate by ice affinity.<sup>150</sup> Initially, it was revealed that the pure extract contained several different molecular weights by MALDI mass spectrometry, indicating that *MaAFPs* (*M. arctica* AFPs) comprised several isoforms. They found that the dominant components of *MaAFPs* were Gly (36 mol%) and Ala (13 mol%), analogous to those of *HhAFPs*. Besides, the *MaAFP* sequence contained 6 tracts of tripeptide repetitive motif Gly-X1-X2, reminiscent of those in *HhAFPs*. Therefore, the researchers predicted that *MaAFPs* also presented amphipathic structures based on the structures of *HhAFPs*. The ice-binding surfaces were mainly composed of hydrophobic residues including Ala, Val and Pro. In contrast, the non-ice binding surfaces contained several charged residues like Lys and Asp, possessing hydrophilic properties.<sup>150</sup> *Granisotoma rainieri* is another kind of springtail that also expresses a Gly-rich AFP with a polyproline type II helix bundle. Distinctly from *HhAFPs* with six or thirteen helices, *GrAFPs* (*G. rainieri* AFPs) contain nine helices being organized into two layers, containing four and five helices, respectively.<sup>151</sup> However, when the researchers explored the homologues of the 3' and 5' UTRs of AFPs by dot matrix analyses, it was depicted that they were highly divergent. As *H. harveyi* and *M. arctica* belong to the same order of Poduromorpha whereas *G. rainieri* is a member of Entomobryomorpha, it was assumed that such

a kind of AFP arose from a common ancestor and HGT events occurred between them.

#### 6.4 HGT-inspired design of antifreeze materials

As noted earlier, HGT events facilitate the transfer of AFP genes between distantly related species, enabling the recipient organism to rapidly acquire antifreeze capabilities. This acquisition significantly enhances its ability to regulate ice growth and recrystallization. Drawing inspiration from this natural process, researchers have extracted advantageous traits of AFPs and incorporated them into the design of novel antifreeze materials, effectively mimicking the HGT process.

For instance, many AFPs have repetitive structural loops to form ice-binding surfaces and each loop contains critical residues that participate in binding to ice crystals. Therefore, Gao *et al.* extracted the functional models from all kinds of AFP sequences to design antifreeze peptides, which exhibited similarities to the mechanisms observed in HGT events (Fig. 11A). As a result, a novel antifreeze peptide AVD was developed, exhibiting excellent IRI activity and significant cell recoveries (95.7% of GLC-82 cells, 3.1 times higher than that without the AVD peptide).<sup>33</sup> This design process is similar to the lateral transfer of herring AFPs into smelts, thus assisting smelts surviving under chilly conditions in nature.<sup>121</sup> Zhang *et al.* obtained a constituent segment “DTASDAAAAAAL” from type I AFPs through the HGT process, which exhibited an  $\alpha$ -helix structure. This segment was successfully employed as coatings, exhibiting excellent anti-icing ability.<sup>152</sup> Overall, these peptide materials retain the functional modules of natural AFPs that bind to ice crystals while discarding other components. Consequently, their stability is enhanced while immunogenicity is reduced, which can better satisfy people's requirements.

Moreover, the HGT-inspired designing method is also considered as the incorporation of a functional domain into an existing material to broaden its application scope. For example, the defects on the substrate tend to induce ice formation because they can increase the absolute value of the adsorption energy of water molecules and cause a higher heat transfer rate.<sup>95</sup> However, anti-icing coatings are typically utilized in extremely cold environments, which can easily cause mechanical damage, resulting in ice nucleation and ice-substrate interlocking.<sup>95</sup> Therefore, Li *et al.* designed an anti-icing coating by incorporating nanoscale fluorinated graphene “horizontally transferred” into a self-healing elastomer, enabling it to maintain its self-healing ability even at an ultralow temperature (–40 °C).<sup>154,155</sup> It was revealed that the defects led to an increase of the ice nucleation temperature ( $T_{IN}$ ) on this anti-icing coating, but the  $T_{IN}$  was restored when the location was self-healed. Moreover, Gao *et al.* “horizontally transferred” a mussel-inspired adhering domain to the N-terminal of *TmAfp*, thus constructing a bifunctional protein with both antifreeze and adhering functions. Furthermore, this bifunctional protein was employed to modify various substrates including glass, plastic and metals, displaying significant anti-icing activity

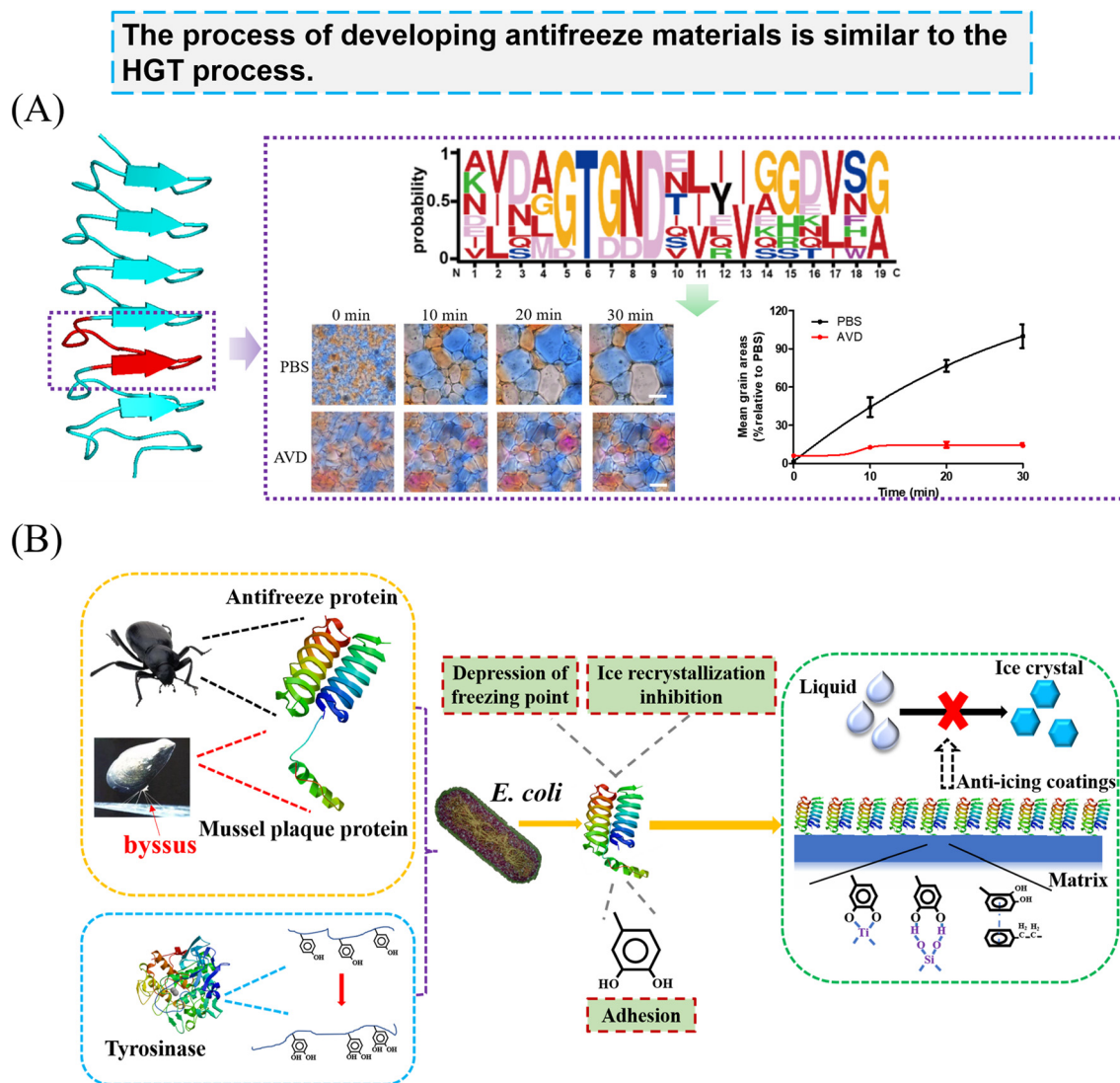


**Fig. 11** (A) The structure of repetitive loops of AFPs. Besides, the conservative analysis was employed to analyze the repetitive sequences of *Mp*AFPs and an AVD peptide was obtained. IRI processes of PBS with or without 5 mg mL<sup>-1</sup> AVD peptide and the corresponding quantification. Reprinted with permission from ref. 33. Copyright (2024) Elsevier. (B) Schematic of the AFP “horizontally transferred” to a mussel plaque protein, thus constituting a chimeric protein possessing both anti-icing and adhesion. Reprinted with permission from ref. 153. Copyright (2022) Elsevier.

(Fig. 11B).<sup>153</sup> These examples all illustrate design methods inspired by the evolutionary process of HGT.

In our opinion, the HGT-inspired design of antifreeze materials can be considered a “modular design strategy” within the scope of engineering strategies. In this process, researchers extracted antifreeze modules from natural AFPs and either employed them directly in practical applications or grafted them onto other polymers. We believe that the designing method presented here can offer valuable inspiration for the future development of novel antifreeze materials.

## 7. Convergent evolution

Convergent evolution generally refers to the process by which two or more independently evolved genes, species, or traits develop similar features or functions under similar

environmental pressures or functional demands, despite their different evolutionary histories. There are mainly two kinds of evolutionary processes of AFPs that involve convergent evolution including type I AFPs and AFGPs.

### 7.1 Type I AFPs

Type I AFPs are extensively distributed across the world, belonging to four superfamilies that are distributed in three different orders (Fig. 12A).<sup>81</sup> Initially, type I AFPs were discovered in winter flounder (order Pleuronectiformes) in 1974.<sup>156</sup> Subsequently, they were found in shorthorn sculpin and snailfish (order Scorpaeniformes).<sup>157,158</sup> Following these discoveries, type I AFPs were also found in cunner (order Perciformes) (Fig. 12A).<sup>159</sup> The four known occurrences of type I AFPs in fish represent separate evolutionary incidents

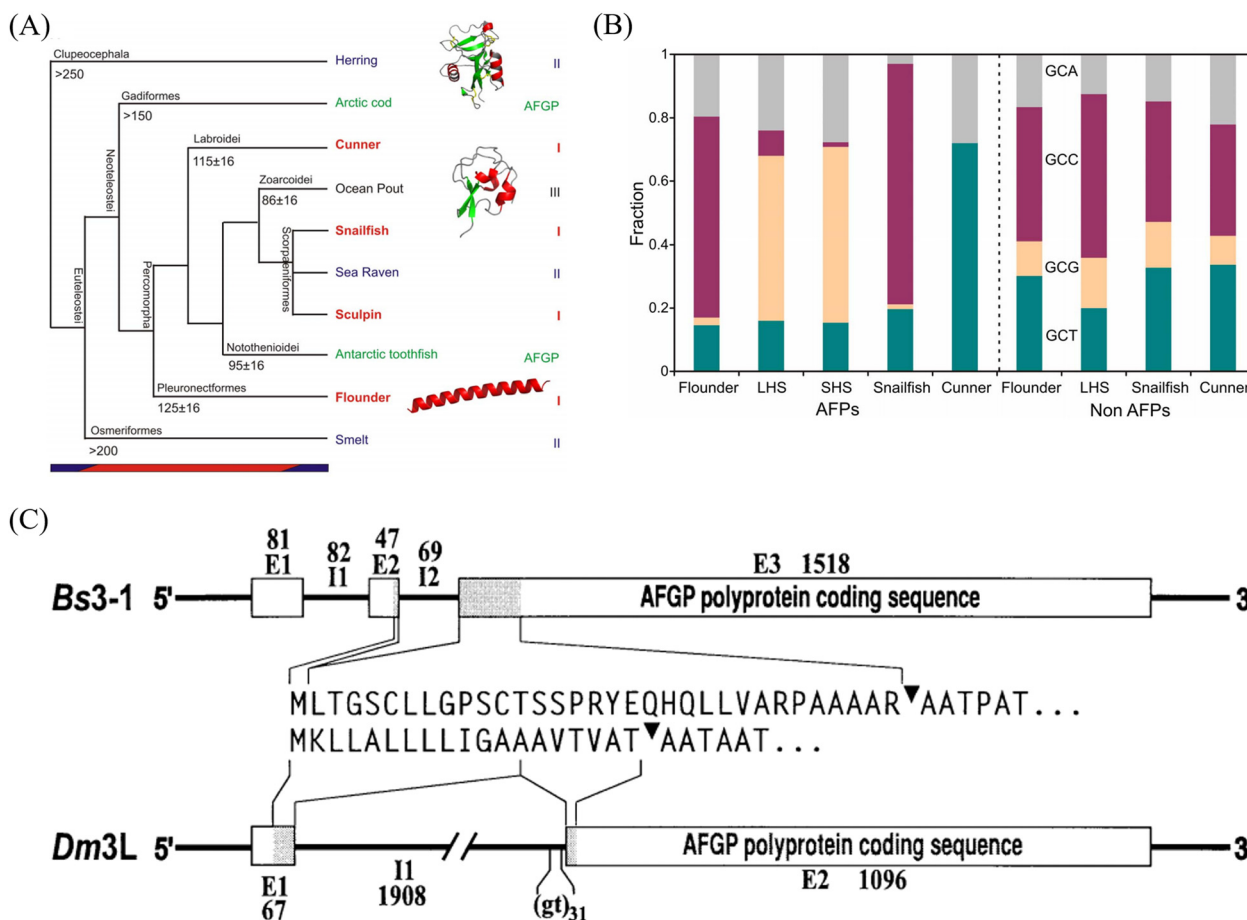


**Fig. 12** (A) The phylogenetic tree of AFP-producing fishes. The name of the organisms producing type I AFPs are marked in red. The name of the organisms producing AFGPs are marked in green. The name of the organisms producing type II AFPs are marked in purple. Reprinted with permission from ref. 81. Copyright (2013) *PLoS One*. (B) The fraction of Ala codon usage of type I AFPs. Reprinted with permission from ref. 81. Copyright (2013) *PLoS One*. (C) The difference between the intron-exon organization of Antarctic notothenioid AFGPs and Arctic codfish AFGPs. Reprinted with permission from ref. 103. Copyright (1997) *Proc. Natl. Acad. Sci. U. S. A.*

that took place shortly following the beginning of the Cenozoic glaciation in the Northern Hemisphere.<sup>82</sup> Within these organisms, type I AFPs exhibit a diverse range of isoforms.<sup>160–163</sup> These different type I AFP isoforms share several similarities: first and foremost, they are all alanine-rich (ranging from 53 mol% in cunner to 71 mol% in shorthorn sculpin) amphipathic proteins, possessing alpha-helical structures. Besides, many type I AFP isoforms share a common 11-residue motif, where the locations of  $i$ ,  $i + 4$ , and  $i + 8$  are occupied by Thr, Ala, and Ala residues, respectively, thus forming an ice-binding surface. Finally, the non-Ala residues adjacent to Thr are generally charged and separated along the helix ( $i$ ,  $i + 4$ ), which serves to stabilize the  $\alpha$ -helix structure of type I AFPs.<sup>81</sup>

However, there are also some differences among different type I AFP isoforms from these four superfamilies.<sup>160–163</sup> They present different lengths, aggregation states and special ranges. These differences strongly suggest that these isoforms have distinct evolutionary origins.<sup>81</sup> First, type I AFPs in sculpin lack introns while those in winter flounder and cunner do have them. Significantly, the location of

introns in winter flounder is markedly different from that in cunner. The intron in cunner is situated in its signal peptide, whereas the intron in winter flounder is located within its coding sequences.<sup>81</sup> Moreover, the UTR regions of these type I AFPs show a lack of similarity.<sup>81</sup> Second, as Ala is the dominant residue of type I AFP sequences, an in-depth investigation into the codon usages of this residue was carried out. It was revealed that the codon usages are species specific. Winter flounder and snailfish prefer GCC (63% and 76%, respectively), sculpin primarily uses GCG (>50%), and cunner tends to employ GCT (>70%) (Fig. 12B).<sup>81</sup> Third, it was revealed that there were no obvious progenitors of type I AFPs through BLAST searches.<sup>81</sup> Building on these findings, it was assumed that type I AFPs among different organisms independently evolved, leading to the occurrence of convergent evolution.<sup>159</sup> Recently, this hypothesis has been confirmed through experimental validation. It was revealed that the AFPs in winter flounder originated from Gig2, a gene that codes for a protein responsible for viral resistance.<sup>164</sup> Besides, the AFP in the sculpin stemmed from lunapark, a gene whose protein resides in the endoplasmic reticulum

and functions to stabilize membrane connections within this organelle.<sup>165</sup> Moreover, the AFPs in the cunner AFP emerged from an alanine-rich area adjacent to the GTPase domain of GIMAPa.<sup>82</sup> However, the AFP gene of the snailfish does not resemble any other known gene loci. These genes all originated from gene duplication and divergence, subsequently undergoing significant expansion in the gene copy number.<sup>82,164,166,167</sup>

## 7.2 AFGPs

Aside from type I AFPs, Antarctic notothenioids and Arctic codfishes both possess AFGPs that also exhibit remarkable similarities. However, these AFGPs have evolved independently (Fig. 12C).<sup>103</sup> There are several lines of evidence supporting this conclusion: first, in terms of their origin at the molecular level, AFGPs in Antarctic notothenioids are derived from a pancreatic trypsinogen. In contrast, AFGPs in Arctic codfishes emerge through *de novo* evolution and have no homology with the pancreatic trypsinogen. Second, polyprotein precursors of AFGPs from Arctic codfishes and Antarctic notothenioids are different. This difference in polyprotein precursors leads to variations in intron–exon organizations and spacers. Third, the coding tripeptide sequences, Thr-Ala(Pro)-Ala, are completely different between Arctic codfish AFGPs and Antarctic notothenioid AFGPs, indicating that they originated from two distinct genes.<sup>103</sup> Collectively, these observations not only establish the independent evolution of AFGPs in Antarctic notothenioids and Arctic codfishes but also provide a classic example of convergent evolution, where similar functional traits (the production of AFGPs) have evolved separately in response to similar environmental pressures (the cold-water habitats of the Antarctic and Arctic regions).

## 7.3 Convergent evolutionary model-inspired design of antifreeze materials

As illustrated, convergent evolution allows unrelated species to independently evolve analogous AFPs in response to similar environmental pressures, such as cold climates. These AFPs often exhibit structural similarities because they collectively address the challenge of modulating ice nucleation, growth, or recrystallization. Consequently, convergent evolution-inspired design antifreeze materials leverage the phenomenon where two or more independently developed materials—particularly antifreeze materials—display structural or functional parallels due to fulfilling analogous roles. By identifying these shared characteristics, researchers can guide the development of innovative antifreeze materials tailored to specific applications.

For instance, an increasing number of anti-icing coatings have been developed in recent years, which can be classified into two categories: low-surface energy coatings and slippery liquid-infused layered coatings. The key mechanisms of anti-icing coatings are to suppress or delay ice formation and reduce ice adhesion, thus preventing ice accumulation on the

surfaces.<sup>168,169</sup> When water remains liquid, the freezing point depression ability should be considered. Once ice crystals have been generated, the ice-phobic ability plays a major function, which is influenced by surface roughness, the flow of a surrounding gas and wettability.<sup>168,170,171</sup>

Understanding the mechanism of anti-icing and icephobicity facilitates the design of low-surface energy coatings and slippery liquid-infused layered coatings. This is because similar functional principles, despite different designs, can converge to produce innovative anti-icing coating solutions. For example, a hydrophilic polyvinylpyrrolidone (PVP)-based polymer has been employed as an anti-icing coating, exhibiting a 34-fold increase in ice delaying time compared to a control.<sup>105</sup> Moreover, SLIPSS also demonstrate excellent anti-icing performances due to their micro/nanostructure that can lock-in a layer of lubricating liquid to protect the surface liquid. A stable lubricant overlayer is maintained through continuous self-replenishment of the surface liquid. For instance, Liu *et al.* prepared three types of SLIPSS using a polytetrafluoroethylene (PTFE)–polyvinylidene fluoride (PVDF) composite membrane infused with three different lubricants: PDMS, ethyl oleate, and perfluoro polyether. The ice adhesion strengths of these SLIPSS were all less than 20 kPa, indicating excellent anti-icing performance. Additionally, they maintained their anti-icing properties after undergoing 10 icing/melting cycles, demonstrating outstanding durability.<sup>172</sup> These design processes are analogous to convergent evolution in nature, where, despite evolving independently, Antarctic and Arctic AFGPs exhibit significant similarities under such cold conditions. This is the inspiration drawn from convergent evolution for material design, where new materials are conceived based on the inevitable commonalities observed in older materials.

In our opinion, the material design approach inspired by convergent evolution primarily illustrates that the strategy involves summarizing design principles from existing materials with similar functions, and subsequently designing new materials based on these extracted principles. This design methodology can be considered “functional simulation and optimization in material design” within the scope of engineering strategies.

## 8. Summary and perspective

Evolutionary biology is a fundamental subject to investigate the genetic origination. AFPs derived from different organisms are independent evolutionary products that undergo the strong-or-death selective pressure of cold, serving as clear exemplary models for investigating the evolutionary process of genes involved in adaptive innovations. In this review, we systematically summarized the main evolutionary models including EAC, *de novo* evolution, HGT and convergent evolutionary models that are involved in the evolution of AFPs and the specific examples of these evolutionary models were introduced. Specifically,

the EAC model suggests that multifunctional AFPs (*i.e.*, type III AFPs and Antarctic AFGPs) evolve through resolving adaptive conflicts. But it should be noted that the empirical support remains limited. *De novo* evolution prompts debates over the relative significance of novel AFP genes emerging from non-coding DNA compared to gene duplication, given its rarity and the still-murky understanding of its underlying mechanisms. HGT accounts for the presence of similar AFPs in evolutionarily distant species (*e.g.*, type II AFPs). However, its detection is still challenging. Convergent evolution elucidates the independent evolution of analogous AFPs (type I AFPs and AFGPs) in unrelated species under similar environmental pressures. However, the genetic mechanisms remain unclear, making it difficult to distinguish true convergence from shared ancestry.

In addition, as natural antifreeze materials, the evolutionary process of AFPs generally follows a trial-and-error approach, which bears similarities to the current development process of novel antifreeze materials. Consequently, we systematically summarized designing methods for antifreeze materials that are analogous to the evolutionary process of natural AFPs. We explicitly mapped the evolutionary insights derived from the EAC model, *de novo* evolution, HGT, and convergent evolution onto corresponding engineering strategies: the function-oriented material design strategy, the integrated design strategy, the modular design strategy, and the functional simulation and optimization strategy in material design, respectively.

These strategies hold great promise for advancing the field of antifreeze material design. They have the potential to inspire the development of more efficient and versatile antifreeze materials, which can then be fine-tuned to adapt to different ambient conditions. For instance, in the industrial field, highly effective antifreeze materials can be developed for anti-icing coatings, thus preventing ice formation and promoting the removal of ice crystals. In the medical field, antifreeze materials contribute to the cryopreservation of all kinds of biological samples including cells, tissues, *etc.* Furthermore, with the continuous exploration of these strategies, we anticipate the discovery of new design principles and the optimization of existing ones, paving the way for breakthroughs in antifreeze material technology.

## Data availability

No primary research results, software or code have been included and no new data were generated or analyzed as part of this review.

## Conflicts of interest

The authors declare no conflicts of interest.

## Acknowledgements

This research was financially supported by the National Key R&D Program of China (Grants 2022YFC2703000), the

National Natural Science Foundation of China (51925307, T2293760, and T2293762), the Strategic Priority Research Program of the Chinese Academy of Sciences (No. XDB1030000), and the Postdoctoral Fellowship Program of CPSF under Grant Number GZC20232771.

## References

- 1 P. Mazur, Freezing of living cells: mechanisms and implications, *Am. J. Physiol.*, 1984, **247**(3 Pt 1), C125–C142.
- 2 K. Muldrew and L. E. McGann, Mechanisms of intracellular ice formation, *Biophys. J.*, 1990, **57**(3), 525–532.
- 3 H. T. Meryman, Cryopreservation of living cells: principles and practice, *Transfusion*, 2007, **47**(5), 935–945.
- 4 P. Mazur, Freezing of Living Cells - Mechanisms and Implications, *Am. J. Physiol.*, 1984, **247**(3), C125–C142.
- 5 F. T. Lynch and A. Khodadoust, Effects of ice accretions on aircraft aerodynamics, *Prog. Aerosp. Sci.*, 2001, **37**(8), 669–767.
- 6 C. C. Liu and J. Liu, Ice Accretion Cause and Mechanism of Glaze on Wires of Power Transmission lines, *Adv. Mater. Res.*, 2011, **189–193**, 3238.
- 7 A. L. Devries and D. E. Wohlschlag, Freezing Resistance in Some Antarctic Fishes, *Science*, 1969, **163**(3871), 1073.
- 8 M. Bar Dolev, I. Braslavsky and P. L. Davies, Ice-Binding Proteins and Their Function, *Annu. Rev. Biochem.*, 2016, **85**, 515–542.
- 9 D. S. Yang, M. Sax, A. Chakrabarty and C. L. Hew, Crystal structure of an antifreeze polypeptide and its mechanistic implications, *Nature*, 1988, **333**(6170), 232–237.
- 10 H. Chao, P. L. Davies, B. D. Sykes and F. D. Sonnichsen, Use of proline mutants to help solve the NMR solution structure of type III antifreeze protein, *Protein Sci.*, 1993, **2**(9), 1411–1428.
- 11 J. G. Duman, Antifreeze and ice nucleator proteins in terrestrial arthropods, *Annu. Rev. Physiol.*, 2001, **63**, 327–357.
- 12 T. Arai, A. Yamauchi, A. Miura, H. Kondo, Y. Nishimiya, Y. C. Sasaki and S. Tsuda, Discovery of Hyperactive Antifreeze Protein from Phylogenetically Distant Beetles Questions Its Evolutionary Origin, *Int. J. Mol. Sci.*, 2021, **22**(7), 3637.
- 13 E. K. Leinala, P. L. Davies, D. Doucet, M. G. Tyshenko, V. K. Walker and Z. Jia, A beta-helical antifreeze protein isoform with increased activity. Structural and functional insights, *J. Biol. Chem.*, 2002, **277**(36), 33349–33352.
- 14 S. R. Sandve, A. Kosmala, H. Rudi, S. Fjellheim, M. Rapacz, T. Yamada and O. A. Rognli, Molecular mechanisms underlying frost tolerance in perennial grasses adapted to cold climates, *Plant Sci.*, 2011, **180**(1), 69–77.
- 15 A. J. Middleton, C. B. Marshall, F. Faucher, M. Bar-Dolev, I. Braslavsky, R. L. Campbell, V. K. Walker and P. L. Davies, Antifreeze Protein from Freeze-Tolerant Grass Has a Beta-Roll Fold with an Irregularly Structured Ice-Binding Site, *J. Mol. Biol.*, 2012, **416**(5), 713–724.
- 16 Y. Wang, L. A. Graham, Z. Han, R. Eves, A. K. Gruneberg, R. L. Campbell, H. Zhang and P. L. Davies, Carrot

- 'antifreeze' protein has an irregular ice-binding site that confers weak freezing point depression but strong inhibition of ice recrystallization, *Biochem. J.*, 2020, **477**(12), 2179–2192.
- 17 J. K. Lee, K. S. Park, S. Park, H. Park, Y. H. Song, S. H. Kang and H. J. Kim, An extracellular ice-binding glycoprotein from an Arctic psychrophilic yeast, *Cryobiology*, 2010, **60**(2), 222–228.
  - 18 S. Q. Guo, C. P. Garnham, J. C. Whitney, L. A. Graham and P. L. Davies, Re-Evaluation of a Bacterial Antifreeze Protein as an Adhesin with Ice-Binding Activity, *PLoS One*, 2012, **7**(11), e48805.
  - 19 H. Xiang, X. Yang, L. Ke and Y. Hu, The properties, biotechnologies, and applications of antifreeze proteins, *Int. J. Biol. Macromol.*, 2020, **153**, 661–675.
  - 20 M. Bar-Dolev, Y. Celik, J. S. Wettlaufer, P. L. Davies and I. Braslavsky, New insights into ice growth and melting modifications by antifreeze proteins, *J. R. Soc., Interface*, 2012, **9**(77), 3249–3259.
  - 21 M. Hassas-Roudsari and H. D. Goff, Ice structuring proteins from plants: Mechanism of action and food application, *Food Res. Int.*, 2012, **46**(1), 425–436.
  - 22 R. C. Deller, M. Vatish, D. A. Mitchell and M. I. Gibson, Synthetic polymers enable non-vitreous cellular cryopreservation by reducing ice crystal growth during thawing, *Nat. Commun.*, 2014, **5**, 3244.
  - 23 Y. F. Zhang, K. Liu, K. Y. Li, V. Gutowski, Y. Yin and J. J. Wang, Fabrication of Anti-Icing Surfaces by Short  $\alpha$ -Helical Peptides, *ACS Appl. Mater. Interfaces*, 2018, **10**(2), 1957–1962.
  - 24 B. Graham, T. L. Bailey, J. R. J. Healey, M. Marcellini, S. Deville and M. I. Gibson, Polyproline as a Minimal Antifreeze Protein Mimic That Enhances the Cryopreservation of Cell Monolayers, *Angew. Chem., Int. Ed.*, 2017, **56**(50), 15941–15944.
  - 25 D. E. Mitchell, G. Clarkson, D. J. Fox, R. A. Vipond, P. Scott and M. I. Gibson, Antifreeze Protein Mimetic Metallohelices with Potent Ice Recrystallization Inhibition Activity, *J. Am. Chem. Soc.*, 2017, **139**(29), 9835–9838.
  - 26 C. A. Stevens, F. Bachtiger, X. D. Kong, L. A. Abriata, G. C. Sosso, M. I. Gibson and H. A. Klok, A minimalistic cyclic ice-binding peptide from phage display, *Nat. Commun.*, 2021, **12**(1), 2675.
  - 27 N. Kalsi, C. Gopalakrishnan, V. Rajendran and R. Purohit, Biophysical aspect of phosphatidylinositol 3-kinase and role of oncogenic mutants (E542K & E545K), *J. Biomol. Struct. Dyn.*, 2016, **34**(12), 2711–2721.
  - 28 B. Kamaraj, V. Rajendran, R. Sethumadhavan and R. Purohit, In-silico screening of cancer associated mutation on PLK1 protein and its structural consequences, *J. Mol. Model.*, 2013, **19**(12), 5587–5599.
  - 29 C. Gopalakrishnan, B. Kamaraj and R. Purohit, Mutations in microRNA Binding Sites of CEP Genes Involved in Cancer, *Cell Biochem. Biophys.*, 2014, **70**(3), 1933–1942.
  - 30 B. Sharma, D. Bhattacharjee, G. Zyryanov and R. Purohit, An insight from computational approach to explore novel, high-affinity phosphodiesterase 10A inhibitors for neurological disorders, *J. Biomol. Struct. Dyn.*, 2023, **41**(19), 9424–9436.
  - 31 A. Kumar, V. Rajendran, R. Sethumadhavan and R. Purohit, Relationship between a point mutation S97C in CK1 $\delta$  protein and its affect on ATP-binding affinity, *J. Biomol. Struct. Dyn.*, 2014, **32**(3), 394–405.
  - 32 B. Kamaraj and R. Purohit, Computational Screening of Disease-Associated Mutations in OCA2 Gene, *Cell Biochem. Biophys.*, 2014, **68**(1), 97–109.
  - 33 H. S. Qi, Y. H. Gao, L. Zhang, Z. X. Cui, X. J. Sui, J. F. Ma, J. Yang, Z. Q. Shu and L. Zhang, Rational Design of and Mechanism Insight into an Efficient Antifreeze Peptide for Cryopreservation, *Engineering*, 2024, **34**, 164–173.
  - 34 H. Y. Geng, X. Liu, G. S. Shi, G. Y. Bai, J. Ma, J. B. Chen, Z. Y. Wu, Y. L. Song, H. P. Fang and J. J. Wang, Graphene Oxide Restricts Growth and Recrystallization of Ice Crystals, *Angew. Chem., Int. Ed.*, 2017, **56**(4), 997–1001.
  - 35 G. Y. Bai, Z. P. Song, H. Y. Geng, D. Gao, K. Liu, S. W. Wu, W. Rao, L. Q. Guo and J. J. Wang, Oxidized Quasi-Carbon Nitride Quantum Dots Inhibit Ice Growth, *Adv. Mater.*, 2017, **29**(28), 1606843.
  - 36 R. M. DeConto, D. Pollard, P. A. Wilson, H. Pälike, C. H. Lear and M. Pagani, Thresholds for Cenozoic bipolar glaciation, *Nature*, 2008, **455**(7213), 652–656.
  - 37 R. M. DeConto and D. Pollard, Rapid Cenozoic glaciation of Antarctica induced by declining atmospheric CO<sub>2</sub>, *Nature*, 2003, **421**(6920), 245–249.
  - 38 J. Zachos, M. Pagani, L. Sloan, E. Thomas and K. Billups, Trends, rhythms, and aberrations in global climate 65 Ma to present, *Science*, 2001, **292**(5517), 686–693.
  - 39 T. J. Near, Estimating divergence times of notothenioid fishes using a fossil-calibrated molecular clock, *Antarct. Sci.*, 2004, **16**(1), 37–44.
  - 40 M. Matschiner, R. Hanel and W. Salzburger, On the Origin and Trigger of the Notothenioid Adaptive Radiation, *PLoS One*, 2011, **6**(4), e18911.
  - 41 T. J. Near, A. Dornburg, K. L. Kuhn, J. T. Eastman, J. N. Pennington, T. Patarnello, L. Zane, D. A. Fernández and C. D. Jones, Ancient climate change, antifreeze, and the evolutionary diversification of Antarctic fishes, *Proc. Natl. Acad. Sci. U. S. A.*, 2012, **109**(9), 3434–3439.
  - 42 N. Eyles, Glacio-epochs and the supercontinent cycle after ~3.0 Ga: Tectonic boundary conditions for glaciation, *Palaeogeogr., Palaeoclimatol., Palaeoecol.*, 2008, **258**(1–2), 89–129.
  - 43 X. Zhuang, C. Yang, K. R. Murphy and C. H. C. Cheng, Molecular mechanism and history of non-sense to sense evolution of antifreeze glycoprotein gene in northern gadids, *Proc. Natl. Acad. Sci. U. S. A.*, 2019, **116**(10), 4400–4405.
  - 44 J. G. Duman, V. Bennett, T. Sformo, R. Hochstrasser and B. M. Barnes, Antifreeze proteins in Alaskan insects and spiders, *J. Insect Physiol.*, 2004, **50**(4), 259–266.
  - 45 J. G. Duman, Animal ice-binding (antifreeze) proteins and glycolipids: an overview with emphasis on physiological function, *J. Exp. Biol.*, 2015, **218**(12), 1846–1855.

- 46 C. H. C. Cheng, L. B. Chen, T. J. Near and Y. M. Jin, Functional antifreeze glycoprotein genes in temperate-water New Zealand nototheniid fish infer an antarctic evolutionary origin, *Mol. Biol. Evol.*, 2003, **20**(11), 1897–1908.
- 47 Y. N. Wang, L. A. Graham, Z. F. Han, R. Eves, A. K. Gruneberg, R. L. Campbell, H. Q. Zhang and P. L. Davies, Carrot 'antifreeze' protein has an irregular ice-binding site that confers weak freezing point depression but strong inhibition of ice recrystallization, *Biochem. J.*, 2020, **477**(12), 2179–2192.
- 48 W. J. Swanson and C. F. Aquadro, Positive Darwinian selection promotes heterogeneity among members of the antifreeze protein multigene family, *J. Mol. Evol.*, 2002, **54**(3), 403–410.
- 49 T. D. R. Vance, M. Bayer-Giraldi, P. L. Davies and M. Mangiagalli, Ice-binding proteins and the 'domain of unknown function' 3494 family, *FEBS J.*, 2019, **286**(5), 855–873.
- 50 P. L. Davies and L. A. Graham, Protein evolution revisited, *Syst. Biol. Reprod. Med.*, 2018, **64**(6), 403–416.
- 51 Y. H. Gao, H. S. Qi and L. Zhang, Advances in Antifreeze Molecules: From Design and Mechanisms to Applications, *Ind. Eng. Chem. Res.*, 2023, **62**(20), 7839–7858.
- 52 A. L. DeVries and D. E. Wohlschlag, Freezing resistance in some Antarctic fishes, *Science*, 1969, **163**(3871), 1073–1075.
- 53 N. F. L. Ng and C. L. Hew, Structure of an Antifreeze Polypeptide from the Sea Raven - Disulfide Bonds and Similarity To Lectin-Binding Proteins, *J. Biol. Chem.*, 1992, **267**(23), 16069–16075.
- 54 A. A. Antson, D. J. Smith, D. I. Roper, S. Lewis, L. S. D. Caves, C. S. Verma, S. L. Buckley, P. J. Lillford and R. E. Hubbard, Understanding the mechanism of ice binding by type III antifreeze proteins, *J. Mol. Biol.*, 2001, **305**(4), 875–889.
- 55 H. J. Kim, J. H. Lee, Y. B. Hur, C. W. Lee, S. H. Park and B. W. Koo, Marine Antifreeze Proteins: Structure, Function, and Application to Cryopreservation as a Potential Cryoprotectant, *Mar. Drugs*, 2017, **15**(2), 27.
- 56 C. Her, Y. Yeh and V. V. Krishnan, The Ensemble of Conformations of Antifreeze Glycoproteins (AFGP8): A Study Using Nuclear Magnetic Resonance Spectroscopy, *Biomolecules*, 2019, **9**(6), 235.
- 57 J. Garner and M. M. Harding, Design and Synthesis of Antifreeze Glycoproteins and Mimics, *ChemBioChem*, 2010, **11**(18), 2489–2498.
- 58 A. P. Tomchaney, J. P. Morris, S. H. Kang and J. G. Duman, Purification, composition, and physical properties of a thermal hysteresis "antifreeze" protein from larvae of the beetle, *Tenebrio molitor*, *Biochemistry*, 1982, **21**(4), 716–721.
- 59 Y. L. Ding, Y. T. Shi and S. H. Yang, Advances and challenges in uncovering cold tolerance regulatory mechanisms in plants, *New Phytol.*, 2019, **222**(4), 1690–1704.
- 60 C. P. Garnham, R. L. Campbell and P. L. Davies, Anchored clathrate waters bind antifreeze proteins to ice, *Proc. Natl. Acad. Sci. U. S. A.*, 2011, **108**(18), 7363–7367.
- 61 T. D. R. Vance, M. Bayer-Giraldi, P. L. Davies and M. Mangiagalli, Ice-binding proteins and the 'domain of unknown function' 3494 family, *FEBS J.*, 2019, **286**(5), 855–873.
- 62 R. Apweiler, A. Bairoch, C. H. Wu, W. C. Barker and L. S. L. Yeh, UniProt: the Universal Protein Knowledgebase, *Nucleic Acids Res.*, 2004, **32**(D1), D115–D119.
- 63 Y. Liu, Z. J. Li, Q. S. Lin, J. Kosinski, J. Seetharaman, J. M. Bujnicki, J. Sivaraman and C. L. Hew, Structure and Evolutionary Origin of Ca-Dependent Herring Type II Antifreeze Protein, *PLoS One*, 2007, **2**(6), e548.
- 64 U. Sorhannus, Evolution of Type II Antifreeze Protein Genes in Teleost Fish: A Complex Scenario Involving Lateral Gene Transfers and Episodic Directional Selection, *Evol. Bioinf. Online*, 2012, **8**, 535–544.
- 65 L. A. Graham, S. C. Loughheed, K. V. Ewart and P. L. Davies, Lateral Transfer of a Lectin-Like Antifreeze Protein Gene in Fishes, *PLoS One*, 2008, **3**(7), e2616.
- 66 J. A. Raymond and H. J. Kim, Possible role of horizontal gene transfer in the colonization of sea ice by algae, *PLoS One*, 2012, **7**(5), e35968.
- 67 C. Deng, C. H. C. Cheng, H. Ye, X. He and L. Chen, Evolution of an antifreeze protein by neofunctionalization under escape from adaptive conflict, *Proc. Natl. Acad. Sci. U. S. A.*, 2010, **107**(50), 21593–21598.
- 68 C. Berthelot, J. Clarke, T. Desvignes, H. W. Detrich, P. Flicek, L. S. Peck, M. Peters, J. H. Postlethwait and M. S. Clark, Adaptation of Proteins to the Cold in Antarctic Fish: A Role for Methionine?, *Genome Biol. Evol.*, 2019, **11**(1), 220–231.
- 69 F. Sievers and D. G. Higgins, Clustal Omega, Accurate Alignment of Very Large Numbers of Sequences, *Methods Mol. Biol.*, 2014, **1079**, 105–116.
- 70 S. Kumar, G. Stecher and K. Tamura, MEGA7: Molecular Evolutionary Genetics Analysis Version 7.0 for Bigger Datasets, *Mol. Biol. Evol.*, 2016, **33**(7), 1870–1874.
- 71 C. Notredame, D. G. Higgins and J. Heringa, T-Coffee: A novel method for fast and accurate multiple sequence alignment, *J. Mol. Biol.*, 2000, **302**(1), 205–217.
- 72 L. B. Chen, A. L. DeVries and C. H. C. Cheng, Evolution of antifreeze glycoprotein gene from a trypsinogen gene in Antarctic nototheniid fish, *Proc. Natl. Acad. Sci. U. S. A.*, 1997, **94**(8), 3811–3816.
- 73 C. H. C. Cheng and L. B. Chen, Evolution of an antifreeze glycoprotein, *Nature*, 1999, **401**(6752), 443–444.
- 74 L. A. Graham, J. Y. Li, W. S. Davidson and P. L. Davies, Smelt was the likely beneficiary of an antifreeze gene laterally transferred between fishes, *BMC Evol. Biol.*, 2012, **12**, 190.
- 75 U. Sorhannus, Evolution of antifreeze protein genes in the diatom genus fragilariopsis: evidence for horizontal gene transfer, gene duplication and episodic diversifying selection, *Evol. Bioinf. Online*, 2011, **7**, 279–289.
- 76 M. Bayer-Giraldi, C. Uhlig, U. John, T. Mock and K. Valentin, Antifreeze proteins in polar sea ice diatoms:

- diversity and gene expression in the genus *Fragilariopsis*, *Environ. Microbiol.*, 2010, **12**(4), 1041–1052.
- 77 C. Uhlig, F. Kilpert, S. Frickenhaus, J. U. Kegel, A. Krell, T. Mock, K. Valentin and B. Beszteri, In situ expression of eukaryotic ice-binding proteins in microbial communities of Arctic and Antarctic sea ice, *ISME J.*, 2015, **9**(11), 2537–2540.
- 78 J. A. Raymond, The ice-binding proteins of a snow alga, *Chloromonas brevispina*: probable acquisition by horizontal gene transfer, *Extremophiles*, 2014, **18**(6), 987–994.
- 79 T. Arai, D. Fukami, T. Hoshino, H. Kondo and S. Tsuda, Ice-binding proteins from the fungus *Antarctomyces psychrotrophicus* possibly originate from two different bacteria through horizontal gene transfer, *FEBS J.*, 2019, **286**(5), 946–962.
- 80 L. A. Graham, W. Qin, S. C. Lougheed, P. L. Davies and V. K. Walker, Evolution of hyperactive, repetitive antifreeze proteins in beetles, *J. Mol. Evol.*, 2007, **64**(4), 387–398.
- 81 L. A. Graham, R. S. Hobbs, G. L. Fletcher and P. L. Davies, Helical Antifreeze Proteins Have Independently Evolved in Fishes on Four Occasions, *PLoS One*, 2013, **8**(12), e81285.
- 82 L. A. Graham and P. L. Davies, Convergent evolution of type I antifreeze proteins from four different progenitors in response to global cooling. *Bmc, Mol. Cell. Biol.*, 2024, **25**(1), 27.
- 83 J. Piatigorsky and G. Wistow, The Recruitment of Crystallins - New Functions Precede Gene Duplication, *Science*, 1991, **252**(5009), 1078–1079.
- 84 A. L. Hughes, The Evolution of Functionally Novel Proteins after Gene Duplication, *Proc. R. Soc. London, Ser. B*, 1994, **256**(1346), 119–124.
- 85 D. L. Des Marais and M. D. Rausher, Escape from adaptive conflict after duplication in an anthocyanin pathway gene, *Nature*, 2008, **454**(7205), 762–765.
- 86 C. T. Hittinger and S. B. Carroll, Gene duplication and the adaptive evolution of a classic genetic switch, *Nature*, 2007, **449**(7163), 677–681.
- 87 Y. Liu, Z. Li, Q. Lin, J. Kosinski, J. Seetharaman, J. M. Bujnicki, J. Sivaraman and C. L. Hew, Structure and evolutionary origin of Ca(2+)-dependent herring type II antifreeze protein, *PLoS One*, 2007, **2**(6), e548.
- 88 C. Deng, C. H. Cheng, H. Ye, X. He and L. Chen, Evolution of an antifreeze protein by neofunctionalization under escape from adaptive conflict, *Proc. Natl. Acad. Sci. U. S. A.*, 2010, **107**(50), 21593–21598.
- 89 Z. Jia, C. I. DeLuca, H. Chao and P. L. Davies, Structural basis for the binding of a globular antifreeze protein to ice, *Nature*, 1996, **384**(6606), 285–288.
- 90 J. Baardsnes and P. L. Davies, Sialic acid synthase: the origin of fish type III antifreeze protein?, *Trends Biochem. Sci.*, 2001, **26**(8), 468–469.
- 91 J. Gunawan, D. Simard, M. Gilbert, A. L. Lovering, W. W. Wakarchuk, M. E. Tanner and N. C. J. Strynadka, Structural and mechanistic analysis of sialic acid synthase NeuB from in complex with Mn phosphoenolpyruvate, and -acetylmannosaminol, *J. Biol. Chem.*, 2005, **280**(5), 3555–3563.
- 92 A. L. DeVries and C. H. C. Cheng, Antifreeze Proteins and Organismal Freezing Avoidance in Polar Fishes, in *Physiology of Polar Fishes*, 2005, pp. 155–201.
- 93 K. Liu, C. L. Wang, J. Ma, G. S. Shi, X. Yao, H. P. Fang, Y. L. Song and J. J. Wang, Janus effect of antifreeze proteins on ice nucleation, *Proc. Natl. Acad. Sci. U. S. A.*, 2016, **113**(51), 14739–14744.
- 94 J. Yang, M. Liu, T. Zhang, J. Ma, Y. Ma, S. Tian, R. Li, Y. Han and L. Zhang, Cell-friendly regulation of ice crystals by antifreeze organism-inspired materials, *AIChE J.*, 2022, **68**(10), e17822.
- 95 S. Tian, R. Li, X. Liu, J. Wang, J. Yu, S. Xu, Y. Tian, J. Yang and L. Zhang, Inhibition of Defect-Induced Ice Nucleation, Propagation, and Adhesion by Bioinspired Self-Healing Anti-Icing Coatings, *Research*, 2023, **6**, 0140.
- 96 J. Yu, S. Tian, G. Lu, S. Xu, K. Yang, L. Ye, Q. Li, L. Zhang and J. Yang, Antifreeze Protein-Inspired Zwitterionic Graphene Oxide Nanosheets for a Photothermal Anti-icing Coating, *Nano Lett.*, 2025, **25**(3), 987–994.
- 97 Y. C. Liou, A. Tocilj, P. L. Davies and Z. C. Jia, Mimicry of ice structure by surface hydroxyls and water of a  $\beta$ -helix antifreeze protein, *Nature*, 2000, **406**(6793), 322–324.
- 98 Q. L. Ye, R. Eves, R. L. Campbell and P. L. Davies, Crystal structure of an insect antifreeze protein reveals ordered waters on the ice-binding surface, *Biochem. J.*, 2020, **477**(17), 3271–3286.
- 99 E. K. Leinala, P. L. Davies, D. Doucet, M. G. Tyshenko, V. K. Walker and Z. C. Jia, A  $\beta$ -helical antifreeze protein isoform with increased activity -: Structural and functional insights, *J. Biol. Chem.*, 2002, **277**(36), 33349–33352.
- 100 W. Zhu, J. M. Guo, J. O. Agola, J. G. Croissant, Z. H. Wang, J. Shang, E. Coker, B. Moteyalli, A. Zimpel, S. Wuttke and C. J. Brinker, Metal-Organic Framework Nanoparticle-Assisted Cryopreservation of Red Blood Cells, *J. Am. Chem. Soc.*, 2019, **141**(19), 7789–7796.
- 101 A. McLysaght and D. Guerzoni, New genes from non-coding sequence: the role of de novo protein-coding genes in eukaryotic evolutionary innovation, *Philos. Trans. R. Soc., B*, 2015, **370**(1678), 20140332.
- 102 C. H. C. Cheng, *Genomic basis for antifreeze glycopeptide heterogeneity and abundance in Antarctic notothenioid fishes*, 1996.
- 103 L. Chen, A. L. DeVries and C. H. Cheng, Convergent evolution of antifreeze glycoproteins in Antarctic notothenioid fish and Arctic cod, *Proc. Natl. Acad. Sci. U. S. A.*, 1997, **94**(8), 3817–3822.
- 104 S. H. Gao, Q. J. Niu, Y. Wang, L. X. Ren, J. H. Chong, K. Y. Zhu and X. Y. Yuan, A Dynamic Membrane-Active Glycopeptide for Enhanced Protection of Human Red Blood Cells against Freeze-Stress, *Adv. Healthcare Mater.*, 2023, **12**(10), 2202516.
- 105 H. S. Guo, M. Liu, C. H. Xie, Y. N. Zhu, X. J. Sui, C. Y. Wen, Q. S. Li, W. Q. Zhao, L. Zhang and J. Yang, A sunlight-responsive and robust anti-icing/deicing coating based on

- the amphiphilic materials, *Chem. Eng. J.*, 2020, **402**, 126161.
- 106 P. G. Chen, S. Tian, H. S. Guo, J. C. Wang, X. M. Liu, S. J. Xu, R. Q. Li, Q. S. Li, C. Y. Wen, J. Yang and L. Zhang, An extreme environment-tolerant anti-icing coating, *Chem. Eng. Sci.*, 2022, **262**, 118010.
- 107 L. Boto, Horizontal gene transfer in evolution: facts and challenges, *Proc. R. Soc. B*, 2010, **277**(1683), 819–827.
- 108 N. Goldenfeld and C. Woese, Biology's next revolution, *Nature*, 2007, **445**(7126), 369–369.
- 109 I. G. Gwak, W. S. Jung, H. J. Kim, S. H. Kang and E. S. Jin, Antifreeze Protein in Antarctic Marine Diatom, *Chaetoceros neogracile*, *Mar. Biotechnol.*, 2010, **12**(6), 630–639.
- 110 R. E. Collins and J. W. Deming, Abundant dissolved genetic material in Arctic sea ice Part I: Extracellular DNA, *Polar Biol.*, 2011, **34**(12), 1819–1830.
- 111 M. G. Lorenz, B. W. Aardema and W. Wackernagel, Highly efficient genetic transformation of *Bacillus subtilis* attached to sand grains, *J. Gen. Microbiol.*, 1988, **134**(1), 107–112.
- 112 M. Bayer-Giraldi, I. Weikusat, H. Besir and G. Dieckmann, Characterization of an antifreeze protein from the polar diatom and its relevance in sea ice, *Cryobiology*, 2011, **63**(3), 210–219.
- 113 K. V. Ewart, B. Rubinsky and G. L. Fletcher, Structural and Functional Similarity Between Fish Antifreeze Proteins and Calcium-Dependent Lectins, *Biochem. Biophys. Res. Commun.*, 1992, **185**(1), 335–340.
- 114 L. A. Graham, S. C. Loughheed, K. V. Ewart and P. L. Davies, Lateral transfer of a lectin-like antifreeze protein gene in fishes, *PLoS One*, 2008, **3**(7), e2616.
- 115 K. Drickamer, C-type lectin-like domains, *Curr. Opin. Struct. Biol.*, 1999, **9**(5), 585–590.
- 116 A. N. Zelensky and J. E. Gready, Comparative analysis of structural properties of the C-type-lectin-like domain (CTLD), *Proteins*, 2003, **52**(3), 466–477.
- 117 U. Sorhannus, Evolution of Type II Antifreeze Protein Genes in Teleost Fish: A Complex Scenario Involving Lateral Gene Transfers and Episodic Directional Selection, *Evol. Bioinf. Online*, 2012, **8**, 535–544.
- 118 K. V. Ewart, B. Rubinsky and G. L. Fletcher, Structural and functional similarity between fish antifreeze proteins and calcium-dependent lectins, *Biochem. Biophys. Res. Commun.*, 1992, **185**(1), 335–340.
- 119 K. V. Ewart and G. L. Fletcher, Herring antifreeze protein: primary structure and evidence for a C-type lectin evolutionary origin, *Mol. Mar. Biol. Biotechnol.*, 1993, **2**(1), 20–27.
- 120 Y. Nishimiya, H. Kondo, M. Takamichi, H. Sugimoto, M. Suzuki, A. Miura and S. Tsuda, Crystal structure and mutational analysis of Ca<sup>2+</sup>-independent type II antifreeze protein from longsnout poacher, *Brachyopsis rostratus*, *J. Mol. Biol.*, 2008, **382**(3), 734–746.
- 121 L. A. Graham, J. Li, W. S. Davidson and P. L. Davies, Smelt was the likely beneficiary of an antifreeze gene laterally transferred between fishes, *BMC Evol. Biol.*, 2012, **12**, 190.
- 122 C. L. Hew, N. C. Wang, S. Joshi, G. L. Fletcher and P. L. Davies, Multiple genes provide the basis for antifreeze protein diversity and dosage in the ocean pout, *Macrozoarces americanus*, *J. Biol. Chem.*, 1988, **263**(24), 12049–12055.
- 123 C. H. C. Cheng and H. W. D. Iii, Molecular Ecophysiology of Antarctic Notothenioid Fishes, *Philos. Trans. R. Soc., B*, 2012, **362**(1488), 355–378.
- 124 P. L. Davies, Conservation of antifreeze protein-encoding genes in tandem repeats, *Gene*, 1992, **112**(2), 163–170.
- 125 L. A. Graham and P. L. Davies, Horizontal Gene Transfer in Vertebrates: A Fishy Tale, *Trends Genet.*, 2021, **37**(6), 501–503.
- 126 T. D. R. Vance, M. Bayer-Giraldi, P. L. Davies and M. Mangiagalli, Ice-binding proteins and the 'domain of unknown function' 3494 family, *FEBS J.*, 2019, **286**(5), 855–873.
- 127 H. Kondo, K. Mochizuki and M. Bayer-Giraldi, Multiple binding modes of a moderate ice-binding protein from a polar microalga, *Phys. Chem. Chem. Phys.*, 2018, **20**(39), 25295–25303.
- 128 M. Bayer-Giraldi, G. Sasaki, K. Nagashima, S. Kipfstuhl, D. A. Vorontsov and Y. Furukawa, Growth suppression of ice crystal basal face in the presence of a moderate ice-binding protein does not confer hyperactivity, *Proc. Natl. Acad. Sci. U. S. A.*, 2018, **115**(29), 7479–7484.
- 129 Y. Hanada, Y. Nishimiya, A. Miura, S. Tsuda and H. Kondo, Hyperactive antifreeze protein from an Antarctic sea ice bacterium *Colwellia* sp. has a compound ice-binding site without repetitive sequences, *FEBS J.*, 2014, **281**(16), 3576–3590.
- 130 H. Do, S. J. Kim, H. J. Kim and J. H. Lee, Structure-based characterization and antifreeze properties of a hyperactive ice-binding protein from the Antarctic bacterium *Flavobacterium frigoris* PS1, *Acta Crystallogr., Sect. D: Biol. Crystallogr.*, 2014, **70**(Pt 4), 1061–1073.
- 131 H. Kondo, Y. Hanada, H. Sugimoto, T. Hoshino, C. P. Garnham, P. L. Davies and S. Tsuda, Ice-binding site of snow mold fungus antifreeze protein deviates from structural regularity and high conservation, *Proc. Natl. Acad. Sci. U. S. A.*, 2012, **109**(24), 9360–9365.
- 132 J. Cheng, Y. Hanada, A. Miura, S. Tsuda and H. Kondo, Hydrophobic ice-binding sites confer hyperactivity of an antifreeze protein from a snow mold fungus, *Biochem. J.*, 2016, **473**(21), 4011–4026.
- 133 J. H. Lee, A. K. Park, H. Do, K. S. Park, S. H. Moh, Y. M. Chi and H. J. Kim, Structural basis for antifreeze activity of ice-binding protein from arctic yeast, *J. Biol. Chem.*, 2012, **287**(14), 11460–11468.
- 134 C. Wang, S. Pakhomova, M. E. Newcomer, B. C. Christner and B. H. Luo, Structural basis of antifreeze activity of a bacterial multi-domain antifreeze protein, *PLoS One*, 2017, **12**(11), e0187169.
- 135 C. Wang, E. E. Oliver, B. C. Christner and B. H. Luo, Functional Analysis of a Bacterial Antifreeze Protein Indicates a Cooperative Effect between Its Two Ice-Binding Domains, *Biochemistry*, 2016, **55**(28), 3975–3983.
- 136 T. Arai, D. Fukami, T. Hoshino, H. Kondo and S. Tsuda, Ice-binding proteins from the fungus possibly originate from two different bacteria through horizontal gene transfer,

- FEBS J.*, 2019, **286**(5), 946–962.
- 137 P. J. Keeling and J. D. Palmer, Horizontal gene transfer in eukaryotic evolution, *Nat. Rev. Genet.*, 2008, **9**(8), 605–618.
- 138 Y. C. Liou, A. Tocilj, P. L. Davies and Z. Jia, Mimicry of ice structure by surface hydroxyls and water of a beta-helix antifreeze protein, *Nature*, 2000, **406**(6793), 322–324.
- 139 S. P. Graether, M. J. Kuiper, S. M. Gagné, V. K. Walker, Z. C. Jia, B. D. Sykes and P. L. Davies,  $\beta$ -helix structure and ice-binding properties of a hyperactive antifreeze protein from an insect, *Nature*, 2000, **406**(6793), 325–328.
- 140 Y. C. Liou, P. Thibault, V. K. Walker, P. L. Davies and L. A. Graham, A complex family of highly heterogeneous and internally repetitive hyperactive antifreeze proteins from the beetle *Tenebrio molitor*, *Biochemistry*, 1999, **38**(35), 11415–11424.
- 141 L. A. Graham, Y. C. Liou, V. K. Walker and P. L. J. N. Davies, Hyperactive antifreeze protein from beetles, *Nature*, 1997, **388**(6644), 727–728.
- 142 J. X. Liu, Y. H. Zhai and J. F. Gui, Molecular characterization and expression pattern of AFP<sub>IV</sub> during embryogenesis in gibel carp (*Carassius auratus gibelio*), *Mol. Biol. Rep.*, 2009, **36**(7), 2011–2018.
- 143 Y. L. Ma, F. Hou and J. Ma, Seasonal changes in cold tolerance of desert beetle *Anatolica polita borealis* (Coleoptera:Tenebrionidae) and their physiological mechanisms, *Kunchong Xuebao*, 2009, **52**(4), 372–379.
- 144 L. M. Qiu, Y. Wang, J. Wang, F. C. Zhang and J. Ma, Expression of biologically active recombinant antifreeze protein His-MpAFP<sub>149</sub> from the desert beetle (*Microdera punctipennis dzungarica*) in *Escherichia coli*, *Mol. Biol. Rep.*, 2010, **37**(4), 1725–1732.
- 145 M. Nei and A. P. Rooney, Concerted and birth-and-death evolution of multigene families, *Annu. Rev. Genet.*, 2005, **39**, 121–152.
- 146 B. L. Pentelute, Z. P. Gates, V. Tereshko, J. L. Dashnau, J. M. Vanderkooi, A. A. Kossiakoff and S. B. H. Kent, X-ray structure of snow flea antifreeze protein determined by racemic crystallization of synthetic protein enantiomers, *J. Am. Chem. Soc.*, 2008, **130**(30), 9695–9701.
- 147 L. A. Graham and P. L. Davies, Glycine-Rich Antifreeze Proteins from Snow Fleas, *Science*, 2005, **310**(5747), 461.
- 148 Y.-F. Mok, F.-H. Lin, L. A. Graham, Y. Celik, I. Braslavsky and P. L. Davies, Structural Basis for the Superior Activity of the Large Isoform of Snow Flea Antifreeze Protein, *FEBS J.*, 2010, **49**(11), 2593–2603.
- 149 S. J. Coulson, I. D. Hodgkinson, A. T. Strathdee, W. Block, N. R. Webb, J. S. Bale and M. R. Worland, Thermal Environments of Arctic Soil Organisms during Winter, *Arct. Alp. Res.*, 1995, **27**(4), 364–370.
- 150 L. A. Graham, M. E. Boddington, M. Holmstrup and P. L. Davies, Antifreeze protein complements cryoprotective dehydration in the freeze-avoiding springtail *Megaphorura arctica*, *Sci. Rep.*, 2020, **10**(1), 3047.
- 151 C. L. T. Scholl, S. Graham, L. A. Davies and L. Peter, Crystal waters on the nine polyproline type II helical bundle springtail antifreeze protein from *Granisotoma rainieri* match the ice lattice, *FEBS J.*, 2021, **288**(14), 4332–4347.
- 152 Y. F. Zhang, K. Liu, K. Y. Li, V. Gutowski, Y. Yin and J. J. Wang, Fabrication of Anti-Icing Surfaces by Short  $\alpha$ -Helical Peptides, *ACS Appl. Mater. Interfaces*, 2018, **10**(2), 1957–1962.
- 153 Y. Gao, H. Qi, D. Fan, J. Yang and L. Zhang, Beetle and mussel-inspired chimeric protein for fabricating anti-icing coating, *Colloids Surf., B*, 2022, **210**, 112252.
- 154 R. Q. Li, S. Tian, Y. Q. Tian, J. C. Wang, S. J. Xu, K. Yang, J. Yang and L. Zhang, An Extreme-Environment-Resistant Self-Healing Anti-Icing Coating, *Small*, 2023, **19**(10), 2206075.
- 155 H. S. Guo, Y. Han, W. Q. Zhao, J. Yang and L. Zhang, Universally autonomous self-healing elastomer with high stretchability, *Nat. Commun.*, 2020, **11**(1), 2037.
- 156 J. G. Duman and A. L. Devries, Freezing Resistance in Winter Flounder *Pseudopleuronectes Americanus*, *Nature*, 1974, **247**(5438), 237–238.
- 157 C. L. Hew, G. L. Fletcher and V. S. Ananthanarayanan, Antifreeze Proteins from the Shorthorn Sculpin, *Myoxocephalus-Scorpius* - Isolation and Characterization, *Can. J. Biochem. Cell Biol.*, 1980, **58**(5), 377–383.
- 158 R. P. Evans and G. L. Fletcher, Isolation and characterization of type I antifreeze proteins from Atlantic snailfish and dusky snailfish, *Biochim. Biophys. Acta, Protein Struct. Mol. Enzymol.*, 2001, **1547**(2), 235–244.
- 159 A. Pastore, L. A. Graham, R. S. Hobbs, G. L. Fletcher and P. L. Davies, Helical Antifreeze Proteins Have Independently Evolved in Fishes on Four Occasions, *PLoS One*, 2013, **8**(12), e81285.
- 160 B. Gourlie, Y. Lin, J. Price, A. L. Devries, D. Powers and R. C. C. Huang, Winter Flounder Antifreeze Proteins - a Multigene Family, *J. Biol. Chem.*, 1984, **259**(23), 4960–4965.
- 161 C. B. Marshall, A. Chakrabarty and P. L. Davies, Hyperactive antifreeze protein from winter flounder is a very long rod-like dimer of  $\alpha$ -helices, *J. Biol. Chem.*, 2005, **280**(18), 17920–17929.
- 162 C. B. Marshall, G. L. Fletcher and P. L. Davies, Hyperactive antifreeze protein in a fish, *Nature*, 2004, **429**(6988), 153.
- 163 Z. Y. Gong, K. V. Ewart, Z. Z. Hu, G. L. Fletcher and C. L. Hew, Skin antifreeze protein genes of the winter flounder, *Pleuronectes americanus*, encode distinct and active polypeptides without the secretory signal and prosequences, *J. Biol. Chem.*, 1996, **271**(8), 4106–4112.
- 164 L. A. Graham, S. Y. Gauthier and P. L. Davies, Origin of an antifreeze protein gene in response to Cenozoic climate change, *Sci. Rep.*, 2022, **12**(1), 8536.
- 165 S. Chen, T. Desai, J. A. McNew, P. Gerard and P. J. Novick, Lunapark stabilizes nascent three-way junctions in the endoplasmic reticulum, *Proc. Natl. Acad. Sci. U. S. A.*, 2015, **112**(2), 418–423.
- 166 C. G. Sun, Y. Liu, Y. S. Hu, Q. D. Fan, W. Li, X. J. Yu, H. L. Mao and C. Y. Hu, Gig1 and Gig2 homologs (CiGig1 and CiGig2) from grass carp () display good antiviral activities in an IFN-independent pathway, *Dev. Comp. Immunol.*,

- 2013, **41**(4), 477–483.
- 167 L. A. Graham and P. L. Davies, Fish antifreeze protein origin in sculpins by frameshifting within a duplicated housekeeping gene, *FEBS J.*, 2024, **291**(18), 4043–4061.
- 168 S. N. Zhang, J. Y. Huang, Y. Cheng, H. Yang, Z. Chen and Y. K. Lai, Bioinspired Surfaces with Superwettability for Anti-Icing and Ice-Phobic Application: Concept, Mechanism, and Design, *Small*, 2017, **13**(48), 1701867.
- 169 J. Y. Lv, Y. L. Song, L. Jiang and J. J. Wang, Bio-Inspired Strategies for Anti-Icing, *ACS Nano*, 2014, **8**(4), 3152–3169.
- 170 J. B. Boreyko and C. P. Collier, Delayed Frost Growth on Jumping-Drop Superhydrophobic Surfaces, *ACS Nano*, 2013, **7**(2), 1618–1627.
- 171 D. K. Sarkar and M. Farzaneh, Superhydrophobic Coatings with Reduced Ice Adhesion, *J. Adhes. Sci. Technol.*, 2009, **23**(9), 1215–1237.
- 172 Y. B. Liu, Y. Tian, J. Chen, H. M. Gu, J. Liu, R. M. Wang, B. L. Zhang, H. P. Zhang and Q. Y. Zhang, Design and preparation of bioinspired slippery liquid-infused porous surfaces with anti-icing performance via delayed phase inversion process, *Colloids Surf., A*, 2020, **588**, 124384.